Bifurcation analysis of elastic residually-stressed circular cylindrical tubes

[1]Andrey Melnikov, [2]*Ray W. Ogden, [3]Luis Dorfmann, [4]Jose Merodio,

[1]Department of Earth Sciences
Memorial University of Newfoundland, St. John's, Canada
melnikov.andrey5@gmail.com

[2]School of Mathematics and Statistics, University of Glasgow
Glasgow G12 8QQ, UK
raymond.ogden@glasgow.ac.uk

[3]Department of Civil and Environmental Engineering, Tufts University
Medford, MA 02155, USA
Luis.Dorfmann@tufts.edu

[4]Department of Continuum Mechanics and Structures
E.T.S. Ing. Caminos, Canales y Puertos
Universidad Politecnica de Madrid, 28040, Madrid, Spain
merodioj@gmail.com

Abstract

The theory of superimposed incremental elastic deformations is applied to a deformed configuration of a residually-stressed circular cylindrical tube. The tube is subject to internal or external pressure and an axial load that maintain its circular cylindrical shape, and then bifurcations from this shape are analyzed. Detailed governing equations and boundary conditions are provided for axisymmetric, prismatic and asymmetric bifurcations for a general form of strain-energy function that incorporates radial and circumferential residual stress components. The theory is applied to a simple model strain-energy function with two material parameters and a parameter that reflects the magnitude of the residual stress. Numerical computations are used to illustrate the dependence of the results of the bifurcation analysis on these parameters and the axial and radial underlying deformation. It is shown that in general the presence of residual stress has a significant effect compared with the corresponding results without residual stress.

Keywords: Nonlinear elasticity; Residual stresses; Incremental elastic deformations; Tube bifurcation.

* Corresponding author.

1 Introduction

Within the context of the theory of nonlinear elasticity the effect of residual stress on material properties and material response has been addressed in recent years in a number of problems. The theory is based on the pioneering work of Hoger (1985, 1986, 1993a,b, 1996) and Johnson and Hoger (1993), with additional contributions from Shams et al. (2011) and Ogden and Singh (2011) related to the effect of initial stress (as distinct from residual stress) on acoustic wave propagation. See also the related papers of Man (1983) and Man and Lu (1987) and the important early work of Biot (1939, 1940).

Residual stresses arise in different materials from causes such as vulcanization in rubberlike materials or during manufacturing (see, for example, Paige, 2002; Paige and Mars, 2004), and in biological tissues during growth and remodelling (see the book by Fung, 1990 for an extensive account). In some cases residual stresses are deliberately induced in order to improve material performance, as, for example, in vehicle windscreens, but residual stresses developed during manufacturing can also cause weakness in the material, deterioration of the material behaviour and reduction in the life of components.

In soft biological tissues, such as arteries and the heart, residual stresses have an enhancing influence on the mechanical response of the tissues during their normal physiological function. For artery walls, the significant effect of inclusion of residual stresses in the constitutive modelling was highlighted in the paper by Holzapfel et al. (2000) based on developing (circumferential and radial) residual stresses from the so-called opening angle method in which a 'stress-free' configuration of a circular arterial sector is closed to form a residually-stressed intact ring (see, also, Rachev, 1997; Rachev and Hayashi, 1999; Ogden, 2003). These papers dealt with the extension and inflation of a circular cylindrical tube representing an artery. As well as circumferential and radial residual stresses, in general axial residual stresses occur, and these were also included in the three-dimensional analysis reported in Holzapfel and Ogden (2010).

The theory based on invariants in Hoger (1993b) has been used for problems involving a circular cylindrical tube by Merodio et al. (2013) (the plane strain problem of azimuthal shear of a tube), by Ogden (2015) (extension and inflation of a fibre-reinforced tube, representing an artery), by Merodio and Ogden (2016) (extension, inflation and torsion of a tube), and by Ahamed et al. (2016) in an application to the effect of residual stresses on the development of an abdominal aortic aneurysm.

It is well known that increasing inflation of a tube of rubberlike material by internal pressure may cause the tube to depart from a circular cylindrical shape. For an elastic material without residual stress this bifurcation behaviour has been analyzed in detail by Haughton and Ogden (1979a,b) for both thin- and thick-walled tubes using the theory of small deformations superimposed on a finite deformation. See also Zhu et al. (2008) and Merodio and Haughton (2010). However, a corresponding analysis that accounts for the presence of residual stress has received little attention in the literature. Exceptions are the papers by Ciarletta et al. (2016), for an unloaded tube, with incremental deformations confined to the cross section of the tube, Du et al. (2019), which analyzes the effect of residual stresses on the development of growth patterns, and Dorfmann and Ogden (2021), for a tube under internal or external pressure and axial load, but also with incremental deformations confined to the cross section of the tube. See also the numerical study Dehghani et al. (2019) where some coupling between different bifurcation modes was

found.

The effect of residual stress on the bifurcation behaviour of a tube has some similarities with the effect of a radial electric field generated by compliant electrodes on its circular boundaries. The latter effect has been examined by Melnikov and Ogden (2018) for prismatic and axisymmetric bifurcations of a neo-Hookean electroelastic constitutive law, and by Dorfmann and Ogden (2019) for axisymmetric bifurcations based on both neo-Hookean and Gent electroelastic constitutive laws. Also, for a neo-Hookean electroelastic constitutive law, axisymmetric vibrations (time-dependent bifurcations) were analyzed in Zhu et al. (2020) within the quasi-electrostatic framework.

In this paper we focus on the bifurcation analysis of a residually-stressed, axially loaded circular cylindrical tube subject to internal or external pressure in order to derive asymmetric, axisymmetric and prismatic bifurcation results, thus generalizing the contribution of Dorfmann and Ogden (2021). The development of such deviations from a finitely deformed circular cylindrical configuration is based on the theory of incremental deformations superimposed on this configuration.

In Section 2 we summarize the basic elements of elasticity with residual stress, including the kinematics of the deformation of a tube subject to radial and axial deformation, and the invariant-based constitutive equations. The theory is then applied in Section 3 to the deformation of a tube, and general formulas for the pressure and axial load required to support the considered deformation are given for a general form of strain-energy function specialized for the considered underlying deformation. This provides a theoretical framework for analyzing the influence of residual stress on the elastic response of a tube irrespective of the particular material model. In order to illustrate the influence of the residual stress a particular form of constitutive model is then selected for purposes of numerical computation. A prototype form of strain-energy function that includes a basic dependence on the residual stress, along with a simple and realistic form of residual stress that mirrors findings from experiments on artery walls, is specified in Section 3.2.

Section 4 provides a summary of the equations governing incremental deformations superimposed on a deformed configuration. These are then specialized in Section 5 for the considered circular cylindrical deformed configuration, and the incremental equations and boundary conditions for general asymmetric incremental bifurcation deformations are derived, with the required lengthy forms of the components of the elasticity tensor listed in Appendix A. The equations are arranged as a first-order system for convenience of numerical computation. The corresponding equations and boundary conditions for both axisymmetric and prismatic bifurcations, which have similar structures but different details, are then given in separate subsections, followed by a summary of the relevant non-dimensionalizations.

In Section 6 numerical results are presented and include comparison with the corresponding results in the absence of residual stresses. Separate subsections detail results for axisymmetric, prismatic and asymmetric bifurcations and illustrate the dependence on the tube geometry, mode number and a measure of residual stress for a radially and axially deformed tube, with material parameters for a specific form of constitutive equation. Reference is made to restrictions imposed by the strong ellipticity condition that have been highlighted in Dorfmann and Ogden (2021).

A short concluding statement is included in Section 7.

2 Basic equations

Consider a material continuum which, when unstressed and unstrained, occupies the *reference* configuration $\mathcal{B}_{\rm r}$. Let a typical material point in this configuration be identified by its position vector $\mathbf{X}$. The continuum is deformed quasi-statically and the corresponding position vector in the deformed configuration $\mathcal{B}$ is denoted $\mathbf{x}$. The deformation from $\mathcal{B}_{\rm r}$ to $\mathcal{B}$ is written $\mathbf{x} = \boldsymbol{\chi}(\mathbf{X})$, where the vector function $\boldsymbol{\chi}$ is referred to as the *deformation*. The deformation gradient tensor, denoted $\mathbf{F}$, is given by $\mathbf{F} = \mathrm{Grad}\boldsymbol{\chi}(\mathbf{X})$, where Grad is the gradient operator with respect to $\mathbf{X}$. The associated right and left Cauchy–Green deformation tensors, denoted $\mathbf{C}$ and $\mathbf{B}$, respectively, are defined by

$$\mathbf{C} = \mathbf{F}^{\rm T}\mathbf{F}, \quad \mathbf{B} = \mathbf{F}\mathbf{F}^{\rm T}, \tag{1}$$

where $^{\rm T}$ signifies the transpose of a second-order tensor.

The principal invariants of $\mathbf{C}$ (equivalently of $\mathbf{B}$), are defined by

$$I_1 = \mathrm{tr}\,\mathbf{C}, \quad I_2 = \frac{1}{2}[(\mathrm{tr}\,\mathbf{C})^2 - \mathrm{tr}\,(\mathbf{C}^2)], \quad I_3 = \det\mathbf{C}. \tag{2}$$

In this paper attention is confined to incompressible materials for which the incompressibility constraint has the form

$$\det\mathbf{F} = 1, \tag{3}$$

and hence $I_3 = 1$.

2.1 Extension and inflation of a tube

We now consider a circular cylindrical tube whose geometry is defined by

$$A \le R \le B, \quad 0 \le \Theta \le 2\pi, \quad 0 \le Z \le L \tag{4}$$

in terms of cylindrical polar coordinates (R, Θ, Z) in the reference configuration $\mathcal{B}_{\rm r}$, where A and B are the internal and external radii and L in the length of the tube. The position vector $\mathbf{X}$ of a point of tube is given by

$$\mathbf{X} = R\mathbf{E}_R + Z\mathbf{E}_Z, \tag{5}$$

where $\mathbf{E}_R$ and $\mathbf{E}_Z$ are the unit basis vectors associated with R and Z, respectively, while $\mathbf{E}_\Theta$ denotes the unit vector associated with Θ.

The corresponding position vector $\mathbf{x}$ in the deformed tube is written

$$\mathbf{x} = r\mathbf{e}_r + z\mathbf{e}_z, \tag{6}$$

where (r, θ, z) are cylindrical polar coordinates in $\mathcal{B}$, which are associated with unit basic vectors $\mathbf{e}_r, \mathbf{e}_\theta, \mathbf{e}_z$, respectively. The tube is subject to axial extension (or contraction) and radial inflation (or deflation) so that the resulting deformation is given by

$$r = \sqrt{a^2 + \lambda_z^{-1}(R^2 - A^2)}, \quad \theta = \Theta, \quad z = \lambda_z Z, \tag{7}$$

where λ_z, a constant, is the axial stretch of the cylinder. The deformed geometry of the tube is given by

$$a \le r \le b, \quad 0 \le \theta \le 2\pi, \quad 0 \le z \le l = \lambda_z L. \tag{8}$$

For this deformation, the deformation gradient is calculated explicitly as

$$\mathbf{F} = \lambda_r \mathbf{e}_r \otimes \mathbf{E}_R + \lambda_\theta \mathbf{e}_\theta \otimes \mathbf{E}_\Theta + \lambda_z \mathbf{e}_z \otimes \mathbf{E}_Z, \tag{9}$$

where λ_r, λ_θ and λ_z are the principal stretches in the radial, azimuthal and axial directions, with $\lambda_\theta = r/R$. The corresponding right and left Cauchy–Green tensors (1) are

$$\mathbf{C} = \lambda_r^2 \mathbf{E}_R \otimes \mathbf{E}_R + \lambda_\theta^2 \mathbf{E}_\Theta \otimes \mathbf{E}_\Theta + \lambda_z^2 \mathbf{E}_Z \otimes \mathbf{E}_Z, \tag{10}$$

$$\mathbf{B} = \lambda_r^2 \mathbf{e}_r \otimes \mathbf{e}_r + \lambda_\theta^2 \mathbf{e}_\theta \otimes \mathbf{e}_\theta + \lambda_z^2 \mathbf{e}_z \otimes \mathbf{e}_z. \tag{11}$$

In terms of the stretches the incompressibility constraint (3) has the form

$$\lambda_r \lambda_\theta \lambda_z = 1, \tag{12}$$

which gives λ_r in terms of the independent stretches λ_z and λ_θ.

2.2 Equilibrium and residual stress

Throughout this paper, we assume that there are no body forces present and no intrinsic couple stresses. The Cauchy stress $\boldsymbol{\sigma}$ (symmetric) and the nominal stress $\mathbf{T}$ then satisfy the equilibrium equations

$$\operatorname{div} \boldsymbol{\sigma} = \mathbf{0}, \quad \operatorname{Div} \mathbf{T} = \mathbf{0}, \tag{13}$$

respectively, where div and Div are the divergence operators with respect to $\mathbf{x} \in \mathcal{B}$ and $\mathbf{X} \in \mathcal{B}_\mathrm{r}$, respectively, and are connected by $\boldsymbol{\sigma} = \mathbf{F}\mathbf{T}$.

If the traction is specified on all or part of the boundary we write the traction boundary condition as

$$\mathbf{T}^\mathrm{T}\mathbf{N} = \mathbf{t}_\mathrm{A} \quad \text{on } \partial\mathcal{B}_\mathrm{r}, \tag{14}$$

where $\mathbf{t}_\mathrm{A}$ is the applied traction per unit area of $\partial\mathcal{B}_\mathrm{r}$ and $\mathbf{N}$ is the unit outward normal on $\partial\mathcal{B}_\mathrm{r}$.

We now assume that the reference configuration $\mathcal{B}_\mathrm{r}$ is residually stressed, with the residual stress tensor denoted by $\boldsymbol{\tau}$. In this configuration, $\mathbf{T} = \boldsymbol{\sigma} = \boldsymbol{\tau}$, i.e. there is no distinction between different measures of stress since the deformation is measured from $\mathcal{B}_\mathrm{r}$. Moreover, as it is assumed that there are no intrinsic couple stresses, $\boldsymbol{\tau}$ is symmetric ($\boldsymbol{\tau}^\mathrm{T} = \boldsymbol{\tau}$) and therefore the rotational balance equations are satisfied in $\mathcal{B}_\mathrm{r}$, where the equilibrium equation

$$\operatorname{Div} \boldsymbol{\tau} = \mathbf{0} \tag{15}$$

is satisfied. By definition of residual stress (see, for example, Hoger, 1985, 1986), the traction should vanish on $\partial\mathcal{B}_\mathrm{r}$, so that

$$\boldsymbol{\tau}\mathbf{N} = \mathbf{0} \quad \text{on } \partial\mathcal{B}_\mathrm{r}. \tag{16}$$

We note in passing that residual stress is a special case of initial stress. For the latter, the boundary traction does not in general vanish. It is important to emphasize that residual stresses are necessarily non-uniform and geometry dependent, and the constitutive law of a residually stressed material body is inhomogeneous.

For the considered circular cylindrical geometry, we assume that the only components of residual stress are τ_{RR}, $\tau_{\Theta\Theta}$, so that $\tau_{ZZ} = 0$ and there is no residual shear stress. The components, τ_{RR} and $\tau_{\Theta\Theta}$ depend only on R, and the equilibrium equation (15) reduces to the radial equation

$$\frac{d\tau_{RR}}{dR} + \frac{1}{R}(\tau_{RR} - \tau_{\Theta\Theta}) = 0, \tag{17}$$

while the boundary condition (16) specializes to

$$\tau_{RR} = 0 \quad \text{on } R = A, B. \tag{18}$$

For given τ_{RR}, $\tau_{\Theta\Theta}$ is determined by (17) as $\mathrm{d}(R\tau_{RR})/\mathrm{d}R$.

2.3 Constitutive equations

For a residually stressed elastic solid, the strain energy is a function of the deformation gradient $\mathbf{F}$ and the residual stress $\boldsymbol{\tau}$, written $W(\mathbf{F}, \boldsymbol{\tau})$ per unit volume. The Cauchy and nominal stress tensors $\boldsymbol{\sigma}$ and $\mathbf{T}$ are given by

$$\boldsymbol{\sigma} = \mathbf{F}\frac{\partial W}{\partial \mathbf{F}}(\mathbf{F}, \boldsymbol{\tau}) - p\mathbf{I}, \quad \mathbf{T} = \frac{\partial W}{\partial \mathbf{F}}(\mathbf{F}, \boldsymbol{\tau}) - p\mathbf{F}^{-1}, \tag{19}$$

where p is a Lagrange multiplier associated with the incompressible constraint (3) and $\mathbf{I}$ is the identity tensor in $\mathcal{B}$. Note that W is automatically objective since $\boldsymbol{\tau}$ is unaffected by rotation in the deformed configuration $\mathcal{B}$ and W depends on $\mathbf{F}$ only via the right Cauchy–Green tensor $\mathbf{C}$ defined in (1). We emphasize that $\boldsymbol{\tau}$ depends on $\mathbf{X}$ and the material is inhomogeneous, and, because of the presence of $\boldsymbol{\tau}$, anisotropic.

When $\mathbf{F} = \mathbf{I}$ the equations in (19) reduce to

$$\boldsymbol{\tau} = \frac{\partial W}{\partial \mathbf{F}}(\mathbf{I}, \boldsymbol{\tau}) - p^{(\mathrm{r})}\mathbf{I}, \tag{20}$$

where $p^{(\mathrm{r})}$ is value of p in $\mathcal{B}_{\mathrm{r}}$. Equation (20) imposes restrictions on the combination of W and $\boldsymbol{\tau}$ that will be made more explicit in the following subsection.

2.3.1 Invariant formulation

Written explicitly as $W(\mathbf{C}, \boldsymbol{\tau})$, W is an isotropic function of the combination of the two tensors $\mathbf{C}$ and $\boldsymbol{\tau}$ according to the theory of Spencer (1971). For an incompressible material, this means that W depends on nine independent invariants of $\mathbf{C}$ and $\boldsymbol{\tau}$ and their combinations. These are typically taken to be (2) for $\mathbf{C}$, as for an isotropic material, but with $I_3 = 1$, for $\boldsymbol{\tau}$,

$$I_4 \equiv \left\{\mathrm{tr}\,\boldsymbol{\tau}, \frac{1}{2}[(\mathrm{tr}\,\boldsymbol{\tau})^2 - \mathrm{tr}\,(\boldsymbol{\tau}^2)], \det\boldsymbol{\tau}\right\}, \tag{21}$$

which are collectively denoted I_4, and, for the invariants involving the combination of $\mathbf{C}$ and $\boldsymbol{\tau}$,

$$I_5 = \mathrm{tr}\,(\boldsymbol{\tau}\mathbf{C}), \quad I_6 = \mathrm{tr}\,(\boldsymbol{\tau}\mathbf{C}^2), \quad I_7 = \mathrm{tr}\,(\boldsymbol{\tau}^2\mathbf{C}), \quad I_8 = \mathrm{tr}\,(\boldsymbol{\tau}^2\mathbf{C}^2), \tag{22}$$

as adopted in Merodio et al. (2013) and Merodio and Ogden (2016), for example.

We now regard W as a function of the nine invariants $(I_1, I_2, I_4, I_5, I_6, I_7, I_8)$. In the following we use the notation $W_i = \partial W/\partial I_i$, $i = 1, 2, 5, 6, 7, 8$. On evaluation of $\partial I_i/\partial \mathbf{F}$, $i = 1, 2, 5, 6, 7, 8$, the Cauchy stress tensor $(19)_1$ then expands out as

$$\begin{aligned}\boldsymbol{\sigma} &= 2W_1\mathbf{B} + 2W_2(I_1\mathbf{B} - \mathbf{B}^2) + 2W_5\boldsymbol{\Sigma} + 2W_6(\boldsymbol{\Sigma}\mathbf{B} + \mathbf{B}\boldsymbol{\Sigma}) \\ &\quad + 2W_7\boldsymbol{\Xi} + 2W_8(\boldsymbol{\Xi}\mathbf{B} + \mathbf{B}\boldsymbol{\Xi}) - p\mathbf{I},\end{aligned} \tag{23}$$

in which we have introduced the notations $\boldsymbol{\Sigma} = \mathbf{F}\boldsymbol{\tau}\mathbf{F}^{\mathrm{T}}$ for the Eulerian tensor which is the push forward of $\boldsymbol{\tau}$ from $\mathcal{B}_{\mathrm{r}}$ to $\mathcal{B}$, and $\boldsymbol{\Xi} = \mathbf{F}\boldsymbol{\tau}^2\mathbf{F}^{\mathrm{T}}$. We also recall that $\mathbf{B} = \mathbf{F}\mathbf{F}^{\mathrm{T}}$ is the left Cauchy–Green tensor.

In the reference configuration $\mathcal{B}_{\mathrm{r}}$ the invariants that depend on $\mathbf{C}$ reduce to

$$I_1 = I_2 = 3, \quad I_5 = I_6 = \mathrm{tr}\,\boldsymbol{\tau}, \quad I_7 = I_8 = \mathrm{tr}(\boldsymbol{\tau}^2). \tag{24}$$

By evaluating (23) in $\mathcal{B}_{\mathrm{r}}$, we obtain the specialization of (20) in the form

$$\boldsymbol{\tau} = (2W_1 + 4W_2 - p^{(\mathrm{r})})\mathbf{I} + 2(W_5 + 2W_6)\boldsymbol{\tau} + 2(W_7 + 2W_8)\boldsymbol{\tau}^2, \tag{25}$$

where all $W_i, i \in \{1, 2, 5, 6, 7, 8\}$, are evaluated for the invariants given by (24). Thus, as in Shams et al. (2011) and Merodio and Ogden (2016), we obtain the residual stress-dependent restrictions

$$2W_1 + 4W_2 - p^{(\mathrm{r})} = 0, \quad 2(W_5 + 2W_6) = 1, \quad W_7 + 2W_8 = 0, \tag{26}$$

on the strain-energy function in $\mathcal{B}_{\mathrm{r}}$.

3 Combined extension and inflation

For the considered deformation, with $\mathbf{C}$ given by (10) and residual stress components τ_{RR} and $\tau_{\Theta\Theta}$, the invariants are given by

$$\begin{aligned}&I_1 = \lambda_r^2 + \lambda_\theta^2 + \lambda_z^2, \quad I_2 = \lambda_\theta^2\lambda_z^2 + \lambda_r^2\lambda_z^2 + \lambda_r^2\lambda_\theta^2, \quad I_4 = \{\tau_{RR} + \tau_{\Theta\Theta}, \tau_{RR}\tau_{\Theta\Theta}\}, \\ &I_5 = \lambda_r^2\tau_{RR} + \lambda_\theta^2\tau_{\Theta\Theta},\ I_6 = \lambda_r^4\tau_{RR} + \lambda_\theta^4\tau_{\Theta\Theta},\ I_7 = \lambda_r^2\tau_{RR}^2 + \lambda_\theta^2\tau_{\Theta\Theta}^2,\ I_8 = \lambda_r^4\tau_{RR}^2 + \lambda_\theta^4\tau_{\Theta\Theta}^2.\end{aligned} \tag{27}$$

They depend on just two independent deformation variables, which we take as λ_θ, λ_z, together with τ_{RR} and $\tau_{\Theta\Theta}$, λ_r being given by the incompressibility condition (12) in terms of λ_θ and λ_z. We therefore write the strain energy as a function of these variables, specifically $\hat{W}(\lambda_\theta, \lambda_z, \tau_{RR}, \tau_{\Theta\Theta})$, which is defined by

$$\hat{W}(\lambda_\theta, \lambda_z, \tau_{RR}, \tau_{\Theta\Theta}) = W(I_1, I_2, I_4, I_5, I_6, I_7, I_8), \tag{28}$$

with $I_1, I_2, I_4, I_5, I_6, I_7, I_8$ given by (27). Then, a straightforward calculation using the appropriate specialization of the components of the Cauchy stress in (23), the expression for $\mathbf{B}$ in (11) and the component matrices of $\boldsymbol{\Sigma}$ and $\boldsymbol{\Xi}$, which have the diagonal forms $\mathrm{diag}[\lambda_r^2\tau_{RR}, \lambda_\theta^2\tau_{\Theta\Theta}, 0]$ and $\mathrm{diag}[\lambda_r^2\tau_{RR}^2, \lambda_\theta^2\tau_{\Theta\Theta}^2, 0]$, respectively, leads to the compact formulas

$$\sigma_{\theta\theta} - \sigma_{rr} = \lambda_\theta\frac{\partial\hat{W}}{\partial\lambda_\theta}, \quad \sigma_{zz} - \sigma_{rr} = \lambda_z\frac{\partial\hat{W}}{\partial\lambda_z}, \tag{29}$$

with $\sigma_{r\theta} = \sigma_{rz} = \sigma_{\theta z} = 0$. These formulas generalize those in the isotropic case, which are recovered on setting the residual stress to zero.

3.1 Equilibrium and applied loads

Since λ_z is a constant and λ_θ depends only on r (equivalently R) and the shear stress components vanish the equilibrium equation $(13)_1$ reduces to one scalar equation, namely

$$r\frac{\mathrm{d}\sigma_{rr}}{\mathrm{d}r} + \sigma_{rr} - \sigma_{\theta\theta} = 0, \tag{30}$$

which can be integrated to give

$$\sigma_{rr} - \sigma_{rr}(a) = \int_a^r (\sigma_{\theta\theta} - \sigma_{rr})\frac{\mathrm{d}r}{r}, \tag{31}$$

where $\sigma_{rr}(a)$ is the value of σ_{rr} on the boundary $r = a$.

We now consider the situation in which the inner surface $r = a$ is subject to a pressure P_a and the outer surface $r = b$ a pressure P_b. Then

$$\sigma_{rr}(a) = -P_a \quad \text{and} \quad \sigma_{rr}(b) = -P_b \tag{32}$$

and, with the help of $(29)_1$, equation (31) becomes

$$P \equiv P_a - P_b = \int_a^b \lambda_\theta \frac{\partial \hat{W}}{\partial \lambda_\theta}\frac{\mathrm{d}r}{r}, \tag{33}$$

which defines the pressure difference P. The overall effective pressure is internal (external) if P is positive (negative).

The axial load N on any cross section is given by

$$N = \int_a^b \int_0^{2\pi} \sigma_{zz} r \mathrm{d}r \mathrm{d}\theta = 2\pi \int_a^b \sigma_{zz} r \mathrm{d}r. \tag{34}$$

On use of (30), the boundary values of σ_{rr} and (29), this leads to an expression for the so-called *reduced axial load* F, which is defined as the total load N on the end of tube with closed ends reduced by the contributions of P_a and P_b. This is given by

$$F \equiv N - \pi a^2 P_a + \pi b^2 P_b = \pi \int_a^b \left(2\lambda_z \frac{\partial \hat{W}}{\partial \lambda_z} - \lambda_\theta \frac{\partial \hat{W}}{\partial \lambda_\theta}\right) r \mathrm{d}r. \tag{35}$$

3.2 A model with residual stress

In order to obtain explicit results we now consider a simple form of energy function, namely

$$W = \frac{1}{2}\mu(I_1 - 3) + \frac{1}{2}(I_5 - \mathrm{tr}\boldsymbol{\tau}) + \frac{1}{4}\kappa(I_5 - \mathrm{tr}\boldsymbol{\tau})^2, \tag{36}$$

where $\mu > 0$ is a constant that corresponds to the shear modulus in the undeformed configuration of a neo-Hookean (isotropic) material (in the absence of residual stress) and κ is a non-negative constant, as introduced in Shams et al. (2011) in a slightly different notation, and also adopted in Merodio et al. (2013) and Merodio and Ogden (2016), for example. Thus, $W = 0$ and $(26)_1$ is satisfied with $p^{(\mathrm{r})} = \mu$ in $\mathcal{B}_\mathrm{r}$. The invariants I_1, I_5 are given in (27).

We note that the term linear in I_5 in (36) provides a very basic dependence of W on the residual stress, but it has limitations. In particular, it was shown in Dorfmann and Ogden (2021) that, with $\kappa = 0$, the restrictions imposed by the strong ellipticity condition are independent of the considered deformation. The term quadratic in I_5 with the coefficient κ removes this limitation in a simple way and provides additional flexibility in the model. This model was also discussed in detail in Shams et al. (2011) and Shams and Ogden (2014) with its implications for acoustic wave propagation. At this point it should be emphasized that because of limited availability of data on residual stress at present it is not appropriate to adopt a more general dependence of W on the residual stress.

The expression (23) for the Cauchy stress simplifies to

$$\boldsymbol{\sigma} = \mu\mathbf{B} + [1 + \kappa(I_5 - \operatorname{tr}\boldsymbol{\tau})]\boldsymbol{\Sigma}, \tag{37}$$

while $\hat{W}(\lambda_\theta, \lambda_z, \tau_{RR}, \tau_{\Theta\Theta})$ becomes

$$\begin{aligned}\hat{W} &= \frac{1}{2}\mu(\lambda_\theta^2 + \lambda_z^2 + \lambda_\theta^{-2}\lambda_z^{-2} - 3) + \frac{1}{2}[(\lambda_\theta^2 - 1)\tau_{\Theta\Theta} + (\lambda_\theta^{-2}\lambda_z^{-2} - 1)\tau_{RR}] \\ &\quad + \frac{1}{4}\kappa[(\lambda_\theta^2 - 1)\tau_{\Theta\Theta} + (\lambda_\theta^{-2}\lambda_z^{-2} - 1)\tau_{RR}]^2,\end{aligned} \tag{38}$$

and the stress differences (29) become

$$\begin{aligned}\lambda_\theta\frac{\partial\hat{W}}{\partial\lambda_\theta} = \sigma_{\theta\theta} - \sigma_{rr} &= \mu(\lambda_\theta^2 - \lambda_\theta^{-2}\lambda_z^{-2}) + \lambda_\theta^2\tau_{\Theta\Theta} - \lambda_\theta^{-2}\lambda_z^{-2}\tau_{RR} \\ &\quad + \kappa[(\lambda_\theta^2 - 1)\tau_{\Theta\Theta} + (\lambda_\theta^{-2}\lambda_z^{-2} - 1)\tau_{RR}](\lambda_\theta^2\tau_{\Theta\Theta} - \lambda_\theta^{-2}\lambda_z^{-2}\tau_{RR}),\end{aligned} \tag{39}$$

$$\begin{aligned}\lambda_z\frac{\partial\hat{W}}{\partial\lambda_z} = \sigma_{zz} - \sigma_{rr} &= \mu(\lambda_z^2 - \lambda_\theta^{-2}\lambda_z^{-2}) - \lambda_\theta^{-2}\lambda_z^{-2}\tau_{RR} \\ &\quad - \kappa[(\lambda_\theta^2 - 1)\tau_{\Theta\Theta} + (\lambda_\theta^{-2}\lambda_z^{-2} - 1)\tau_{RR}]\lambda_\theta^{-2}\lambda_z^{-2}\tau_{RR}.\end{aligned} \tag{40}$$

In conjunction with these models it suffices to adopt a specific form of the residual stress component τ_{RR} that satisfies the boundary conditions (18). We therefore choose the simple form

$$\tau_{RR} = \nu(R - A)(R - B), \tag{41}$$

as introduced in Merodio et al. (2013), where ν is constant which defines the magnitude of the residual stress. We note that $\tau_{RR} < 0\,(> 0)$ for $\nu > 0\,(< 0)$. This form reflects very closely the nature of the radial residual stress in artery walls as determined by the opening angle experiment (see, for example, Ogden, 2003 for discussion of the background). It follows from (17) that $\tau_{\Theta\Theta}$ is given by

$$\tau_{\Theta\Theta} = \nu[3R^2 - 2(A + B)R + AB]. \tag{42}$$

Based on the formula for P in (33), for fixed λ_z, plots of the dimensionless pressure versus $\lambda_a = a/A$ that illustrate the dependence on both ν and κ (in dimensionless form) have been provided in Dorfmann and Ogden (2021) for the representative ratio $B/A = 1.2$. Similarly, for $\kappa = 0$ plots of dimensionless pressure that illustrate the dependence on both ν and B/A are included in Ogden (2015), which also provides illustrations of the dependence of the reduced axial load F on these parameters.

4 Incremental equations

In this section we summarize the equations governing incremental deformations superimposed on a deformed configuration. A more detailed discussion of this theory can be found in Ogden (1997).

We consider a small displacement of the deformed position $\mathbf{x}$, i.e. an increment, denoted $\dot{\mathbf{x}}$, and the corresponding increment $\dot{\mathbf{F}} = \mathrm{Grad}\,\dot{\mathbf{x}}$ in the deformation gradient. Other incremental quantities are likewise indicated by a superimposed dot, including the incremental nominal stress $\dot{\mathbf{T}}$, which satisfies the incremental equilibrium equation

$$\mathrm{Div}\,\dot{\mathbf{T}} = \mathbf{0}, \tag{43}$$

and the associated incremental form of the boundary condition (14) is

$$\dot{\mathbf{T}}^{\mathrm{T}}\mathbf{N} = \dot{\mathbf{t}}_{\mathrm{A}} \quad \text{on } \partial\mathcal{B}_{\mathrm{r}}, \tag{44}$$

per unit area of $\partial\mathcal{B}_{\mathrm{r}}$.

We now work in terms of the push-forward version of the increment $\dot{\mathbf{T}}$ defined by $\dot{\mathbf{T}}_0 = \mathbf{F}\dot{\mathbf{T}}$, which satisfies the equilibrium equation equivalent to (43), i.e.

$$\mathrm{div}\,\dot{\mathbf{T}}_0 = \mathbf{0}, \tag{45}$$

and the corresponding boundary condition

$$\dot{\mathbf{T}}_0^{\mathrm{T}}\mathbf{n} = \dot{\mathbf{t}}_{\mathrm{A0}} \quad \text{on } \partial\mathcal{B}, \tag{46}$$

per unit area of $\partial\mathcal{B}$. The subscript $_0$ signifies a push forward quantity here and subsequently.

The incremental form of the incompressibility condition (3) becomes

$$\mathrm{tr}\,\mathbf{L} \equiv \mathrm{div}\,\mathbf{u} = 0, \tag{47}$$

where $\mathbf{L} = \dot{\mathbf{F}}\mathbf{F}^{-1} = \mathrm{grad}\,\mathbf{u}$ is the displacement gradient, $\mathbf{u}\,(= \dot{\mathbf{x}})$ being a function of $\mathbf{x}$.

Let $\mathbf{e}_1$, $\mathbf{e}_2$, $\mathbf{e}_3$ be unit basis vectors in an orthogonal curvilinear coordinate system. Then, in component form, equation (45) yields the three scalar equations

$$\dot{T}_{0ji,j} + \dot{T}_{0ji}\mathbf{e}_k \cdot \mathbf{e}_{j,k} + \dot{T}_{0kj}\mathbf{e}_i \cdot \mathbf{e}_{j,k} = 0, \quad i = 1, 2, 3, \tag{48}$$

in which summation over repeated indices j and k from 1 to 3 is implied and the notation $_{,j}$ represents the derivative associated with the jth curvilinear coordinate, and is made explicit in Section 5 for cylindrical polar coordinates.

4.1 Incremental constitutive equations

The increment $\dot{\mathbf{F}}$ induces an increment $\dot{\mathbf{T}}$ in the nominal stress, leading to the following (linearized) incremental form of the constitutive law. By forming the increment of $(19)_2$ and using $\dot{\overline{\mathbf{F}^{-1}}} = -\mathbf{F}^{-1}\dot{\mathbf{F}}\mathbf{F}^{-1}$, we obtain

$$\dot{\mathbf{T}} = \boldsymbol{\mathcal{A}}\dot{\mathbf{F}} + p\mathbf{F}^{-1}\dot{\mathbf{F}}\mathbf{F}^{-1} - \dot{p}\mathbf{F}^{-1}, \tag{49}$$

where $\boldsymbol{\mathcal{A}}$, which is a fourth-order tensor, denotes the elastic modulus tensor associated with the strain-energy function W. Its component form, along with its symmetries, is written

$$\mathcal{A}_{\alpha i\beta j} = \frac{\partial^2 W}{\partial F_{i\alpha}\partial F_{j\beta}}, \quad \mathcal{A}_{\alpha i\beta j} = \mathcal{A}_{\beta j\alpha i}. \tag{50}$$

The updated version of (49) is

$$\dot{\mathbf{T}}_0 = \boldsymbol{\mathcal{A}}_0\mathbf{L} + p\mathbf{L} - \dot{p}\mathbf{I}, \tag{51}$$

where $\boldsymbol{\mathcal{A}}_0$ is the push forward version of $\boldsymbol{\mathcal{A}}$ with components related to those of $\boldsymbol{\mathcal{A}}$ by

$$\mathcal{A}_{0lkji} = \mathcal{A}_{0jilk} = F_{j\alpha}F_{l\beta}\mathcal{A}_{\alpha i\beta k}. \tag{52}$$

In terms of invariants the updated elasticity tensor has the expanded component form

$$\mathcal{A}_{0piqj} = \sum_{r\in\mathcal{I}} W_r F_{p\alpha}F_{q\beta}\frac{\partial^2 I_r}{\partial F_{i\alpha}\partial F_{j\beta}} + \sum_{r,s\in\mathcal{I}} W_{rs}F_{p\alpha}F_{q\beta}\frac{\partial I_r}{\partial F_{i\alpha}}\frac{\partial I_s}{\partial F_{j\beta}}, \tag{53}$$

where $W_{rs} = \partial^2 W/\partial I_r \partial I_s$ and $\mathcal{I}$ is the index set $\{1, 2, 5, 6, 7, 8\}$. The full expansion of $\mathcal{A}_{0piqj}$ in terms of invariants is given in Appendix A.

We also record here the useful connection

$$\mathcal{A}_{0jisk} - \mathcal{A}_{0ijsk} = (\sigma_{js} + p\delta_{js})\delta_{ik} - (\sigma_{is} + p\delta_{is})\delta_{jk}, \tag{54}$$

which is a consequence of the incremental version of the symmetry condition $(\mathbf{FT})^{\mathrm{T}} = \mathbf{FT} = \boldsymbol{\sigma}$.

5 Bifurcation of a residually stressed circular cylinder

In this section, for consistency with the corresponding analysis in Haughton and Ogden (1979b) in which there is no residual stress, we re-order the coordinates r, θ, z as θ, z, r, associated with the stretches $\lambda_\theta, \lambda_z, \lambda_r$, respectively. The unit basis vectors associated with the cylindrical polar coordinates θ, z, r are denoted $\mathbf{e}_1$, $\mathbf{e}_2$, $\mathbf{e}_3$, and the derivatives $(\cdot)_{,k}$ in (48) denoted by subscripts with commas become $\partial/r\partial\theta$, $\partial/\partial z$, $\partial/\partial r$ for $k = 1, 2, 3$, respectively. For the cylindrical polar coordinates the only non-zero scalar products $\mathbf{e}_i\cdot\mathbf{e}_{j,k}$ in (48) are

$$\mathbf{e}_1 \cdot \mathbf{e}_{3,1} = -\mathbf{e}_3 \cdot \mathbf{e}_{1,1} = 1/r. \tag{55}$$

The incremental displacement $\dot{\mathbf{x}} = \mathbf{u}$ is written

$$\mathbf{u} = v\mathbf{e}_1 + w\mathbf{e}_2 + u\mathbf{e}_3, \tag{56}$$

and the matrix of components of $\mathbf{L} = \operatorname{grad}\mathbf{u}$ with respect to the basis vectors $\mathbf{e}_1, \mathbf{e}_2, \mathbf{e}_3$ is

$$[L_{ij}] = \begin{bmatrix} (u + v_\theta)/r & v_z & v_r \\ w_\theta/r & w_z & w_r \\ (u_\theta - v)/r & u_z & u_r \end{bmatrix}, \tag{57}$$

where the subscripts θ, z, r without a preceding comma indicate the corresponding partial derivatives.

The incremental incompressibility condition (47) specializes to

$$L_{11} + L_{22} + L_{33} \equiv (u + v_\theta)/r + w_z + u_r = 0. \tag{58}$$

We emphasize that from now on we adopt the indices $1, 2, 3$ instead of θ, z, r, respectively, for the components of tensors.

5.1 Asymmetric bifurcations

From (48) and (55) the governing equations for $i = 1, 2, 3$ can be obtained as

$$\dot{T}_{011,1} + \dot{T}_{021,2} + \dot{T}_{031,3} + (\dot{T}_{031} + \dot{T}_{013})/r = 0, \tag{59}$$

$$\dot{T}_{012,1} + \dot{T}_{022,2} + \dot{T}_{032,3} + \dot{T}_{032}/r = 0, \tag{60}$$

$$\dot{T}_{013,1} + \dot{T}_{023,2} + \dot{T}_{033,3} + (\dot{T}_{033} - \dot{T}_{011})/r = 0. \tag{61}$$

For the considered underlying cylindrical configuration the components of $\dot{\mathbf{T}}_0$ in the three equations above are given by

$$\dot{T}_{011} = (\mathcal{A}_{01111} + p)L_{11} + \mathcal{A}_{01122}L_{22} + \mathcal{A}_{01133}L_{33} - \dot{p}, \tag{62}$$

$$\dot{T}_{022} = \mathcal{A}_{01122}L_{11} + (\mathcal{A}_{02222} + p)L_{22} + \mathcal{A}_{02233}L_{33} - \dot{p}, \tag{63}$$

$$\dot{T}_{033} = \mathcal{A}_{01133}L_{11} + \mathcal{A}_{02233}L_{22} + (\mathcal{A}_{03333} + p)L_{33} - \dot{p}, \tag{64}$$

$$\dot{T}_{012} = \mathcal{A}_{01212}L_{21} + (\mathcal{A}_{01221} + p)L_{12}, \quad \dot{T}_{021} = \mathcal{A}_{02121}L_{12} + (\mathcal{A}_{01221} + p)L_{21}, \tag{65}$$

$$\dot{T}_{013} = \mathcal{A}_{01313}L_{31} + (\mathcal{A}_{01331} + p)L_{13}, \quad \dot{T}_{031} = \mathcal{A}_{03131}L_{13} + (\mathcal{A}_{01331} + p)L_{31}, \tag{66}$$

$$\dot{T}_{023} = \mathcal{A}_{02323}L_{32} + (\mathcal{A}_{02332} + p)L_{23}, \quad \dot{T}_{032} = \mathcal{A}_{03232}L_{23} + (\mathcal{A}_{02332} + p)L_{32}, \tag{67}$$

where the components of the tensor $\boldsymbol{\mathcal{A}}_0$ are obtained by specializing the general expressions given in Appendix A.

On substitution of these expressions into (59)–(61) and use of the incompressibility condition (58), we obtain

$$\begin{aligned}\dot{p}_\theta &= (r\mathcal{A}'_{03131} + \mathcal{A}_{03131})(u_\theta + rv_r - v)/r + (\mathcal{A}_{01111} - \mathcal{A}_{01122} - \mathcal{A}_{02112})(u_\theta + v_{\theta\theta})/r \\ &\quad + \mathcal{A}_{02121}rv_{zz} + \mathcal{A}_{03131}rv_{rr} + (\mathcal{A}_{01133} - \mathcal{A}_{01122} - \mathcal{A}_{02112} + \mathcal{A}_{03113})u_{r\theta},\end{aligned} \tag{68}$$

$$\begin{aligned}\dot{p}_z &= (r\mathcal{A}'_{03232} + \mathcal{A}_{03232})(u_z + w_r)/r + \mathcal{A}_{01212}(w_{\theta\theta} - ru_z)/r^2 + \mathcal{A}_{03232}w_{rr} \\ &\quad + (\mathcal{A}_{02222} - \mathcal{A}_{01221} - \mathcal{A}_{01122})w_{zz} + (\mathcal{A}_{02233} + \mathcal{A}_{03223} - \mathcal{A}_{01221} - \mathcal{A}_{01122})u_{rz},\end{aligned} \tag{69}$$

$$\begin{aligned}\dot{p}_r &= \mathcal{A}_{01313}(u_{\theta\theta} - v_\theta)/r^2 + (r\mathcal{A}'_{01133} - r\mathcal{A}'_{02233} - \mathcal{A}_{01111} + \mathcal{A}_{01122} + \mathcal{A}_{03223})(v_\theta + u)/r^2 \\ &\quad + (\mathcal{A}_{01331} + \mathcal{A}_{01133} - \mathcal{A}_{03223} - \mathcal{A}_{02233})v_{r\theta}/r + (\mathcal{A}_{03333} - \mathcal{A}_{02233} - \mathcal{A}_{03223})u_{rr} \\ &\quad + \mathcal{A}_{02323}u_{zz} + (r\mathcal{A}'_{03333} - r\mathcal{A}'_{02233} + rp' + \mathcal{A}_{03333} - 2\mathcal{A}_{02233} + \mathcal{A}_{01122} - \mathcal{A}_{03223})u_r/r,\end{aligned} \tag{70}$$

respectively, where a prime signifies differentiation with respect to r.

Note that, on use of the connections $\mathcal{A}_{03131} - \mathcal{A}_{01331} = \sigma_{33} + p$ and $\mathcal{A}_{01313} - \mathcal{A}_{03131} = \sigma_{11} - \sigma_{33}$ from (54) and the equilibrium equation (30) in the form $r\sigma'_{33} = \sigma_{11} - \sigma_{33}$, we have

$$rp' = r\mathcal{A}'_{03131} - r\mathcal{A}'_{01331} + \mathcal{A}_{03131} - \mathcal{A}_{01313}. \tag{71}$$

For pressure loading, the boundary condition (46) is specialized to $\dot{\mathbf{T}}_0^{\mathrm{T}}\mathbf{n} = \dot{\mathbf{t}}_{\mathrm{A}0} = P\mathbf{L}^{\mathrm{T}}\mathbf{n} - \dot{P}\mathbf{n}$ on $\partial\mathcal{B}$, where $\mathbf{n}$ is the unit outward normal to $\partial\mathcal{B}$ and $\dot{P}$ is a pressure increment, which we set to zero on each boundary $r = a$ and $r = b$. Thus,

$$\dot{\mathbf{T}}_0^{\mathrm{T}}\mathbf{n} = \begin{cases} P_a\mathbf{L}^{\mathrm{T}}\mathbf{n} & \text{on } r = a \\ P_b\mathbf{L}^{\mathrm{T}}\mathbf{n} & \text{on } r = b, \end{cases} \qquad \dot{T}_{03i} = \begin{cases} P_a L_{3i} & \text{on } r = a \\ P_b L_{3i} & \text{on } r = b, \end{cases} \tag{72}$$

for $i = 1, 2, 3$.

We assume that $\mathcal{A}_{03131} \neq 0$, $\mathcal{A}_{03232} \neq 0$. Then, by using (32), (54), $(66)_2$, $(67)_2$ and the boundary conditions (72) for $i = 1, 2$ become

$$L_{13} + L_{31} = 0, \quad L_{23} + L_{32} = 0 \quad \text{on } r = a, b, \tag{73}$$

while for $i = 3$, on use of (32), (54) and (64), we obtain

$$\mathcal{A}_{01133}L_{11} + \mathcal{A}_{02233}L_{22} + (\mathcal{A}_{03333} + \mathcal{A}_{03131} - \mathcal{A}_{01331})L_{33} - \dot{p} = 0 \quad \text{on } r = a, b. \tag{74}$$

We now consider the Ansätze

$$\begin{aligned} u &= f(r)\cos m\theta\cos\alpha z, \quad v = g(r)\sin m\theta\cos\alpha z, \\ w &= h(r)\cos m\theta\sin\alpha z, \quad \dot{p} = k(r)\cos m\theta\cos\alpha z, \end{aligned} \tag{75}$$

where m is a non-negative integer and α is a non-negative constant. From the incompressibility condition (58) we then obtain

$$h(r) = -\frac{rf'(r) + f(r) + mg(r)}{\alpha r}. \tag{76}$$

Substituting expressions (75) into (68)–(70) and eliminating $h(r)$ using (76) we obtain the governing equations

$$\begin{aligned} &(r\mathcal{A}'_{03131} + \mathcal{A}_{03131} + \mathcal{A}_{01111} - \mathcal{A}_{01122} - \mathcal{A}_{02112})mf(r) \\ &+ (\mathcal{A}_{01133} - \mathcal{A}_{01122} - \mathcal{A}_{02112} + \mathcal{A}_{03113})rmf'(r) \\ &+ [r\mathcal{A}'_{03131} + \mathcal{A}_{03131} + m^2(\mathcal{A}_{01111} - \mathcal{A}_{01122} - \mathcal{A}_{02112}) + \alpha^2r^2\mathcal{A}_{02121}]g(r) \\ &- (r\mathcal{A}'_{03131} + \mathcal{A}_{03131})rg'(r) - r^2g''(r)\mathcal{A}_{03131} - mrk(r) = 0, \end{aligned} \tag{77}$$

$$\begin{aligned} &[r\mathcal{A}'_{03232} - \mathcal{A}_{03232} + m^2\mathcal{A}_{01212} \\ &- \alpha^2r^2(r\mathcal{A}'_{03232} + \mathcal{A}_{03232} - \mathcal{A}_{01212} - \mathcal{A}_{02222} + \mathcal{A}_{01221} + \mathcal{A}_{01122})]f(r) \\ &- [r\mathcal{A}'_{03232} - \mathcal{A}_{03232} - m^2\mathcal{A}_{01212} - \alpha^2r^2(\mathcal{A}_{02222} - \mathcal{A}_{02233} - \mathcal{A}_{03223})]rf'(r) \\ &- (r\mathcal{A}'_{03232} + 2\mathcal{A}_{03232})r^2f''(r) - \mathcal{A}_{03232}r^3f'''(r) \\ &+ [r\mathcal{A}'_{03232} - \mathcal{A}_{03232} + m^2\mathcal{A}_{01212} + \alpha^2r^2(\mathcal{A}_{02222} - \mathcal{A}_{01221} - \mathcal{A}_{01122})]mg(r) \\ &- (r\mathcal{A}'_{03232} - \mathcal{A}_{03232})mrg'(r) - \mathcal{A}_{03232}mr^2g''(r) + \alpha^2r^3k(r) = 0, \end{aligned} \tag{78}$$

$$\begin{aligned} &(r\mathcal{A}'_{01133} - r\mathcal{A}'_{02233} - \mathcal{A}_{01111} + \mathcal{A}_{01122} + \mathcal{A}_{03223} - \alpha^2r^2\mathcal{A}_{02323} - m^2\mathcal{A}_{01313})f(r) \\ &+ (r\mathcal{A}'_{03333} - r\mathcal{A}'_{02233} + rp' + \mathcal{A}_{03333} - 2\mathcal{A}_{02233} + \mathcal{A}_{01122} - \mathcal{A}_{03223})rf'(r) \\ &+ (\mathcal{A}_{03333} - \mathcal{A}_{02233} - \mathcal{A}_{03223})r^2f''(r) \\ &+ (r\mathcal{A}'_{01133} - r\mathcal{A}'_{02233} - \mathcal{A}_{01111} + \mathcal{A}_{01122} + \mathcal{A}_{03223} - \mathcal{A}_{01313})mg(r) \\ &+ (\mathcal{A}_{01331} + \mathcal{A}_{01133} - \mathcal{A}_{03223} - \mathcal{A}_{02233})mrg'(r) - r^2k'(r) = 0. \end{aligned} \tag{79}$$

Using (57) and (75), the boundary condition $(73)_1$ becomes

$$mf(r) - rg'(r) + g(r) = 0 \quad \text{on } r = a, b, \tag{80}$$

and using (57) and (75) with the help of (76) and (80), the boundary condition $(73)_2$ can be rewritten as

$$r^2 f''(r) + rf'(r) + (\alpha^2 r^2 + m^2 - 1)f(r) = 0 \quad \text{on } r = a, b. \tag{81}$$

The boundary condition (74) becomes, on use of (57), (58) and (75),

$$\begin{aligned}(\mathcal{A}_{03333} + \mathcal{A}_{03131} - \mathcal{A}_{01331} - \mathcal{A}_{02233})rf'(r) \,+\, &(\mathcal{A}_{01133} - \mathcal{A}_{02233})[f(r) + mg(r)] \\ &- rk(r) = 0 \quad \text{on } r = a, b.\end{aligned} \tag{82}$$

We now arrange the set of equations and boundary conditions above as a first-order system by introducing the notation

$$y_1 = f(r), \quad y_2 = f'(r), \quad y_3 = f''(r), \quad y_4 = g(r), \quad y_5 = g'(r), \quad y_6 = k(r), \tag{83}$$

and forming the array $\mathbf{y} = (y_1, y_2, y_3, y_4, y_5, y_6)$. The system can then be written compactly in the form

$$\mathbf{y}' = \mathbf{M}\mathbf{y}, \tag{84}$$

where $\mathbf{M}$ is a 6×6 matrix of the form

$$\mathbf{M} = \begin{bmatrix} 0 & 1 & 0 & 0 & 0 & 0 \\ 0 & 0 & 1 & 0 & 0 & 0 \\ \mathsf{M}_{31} & \mathsf{M}_{32} & \mathsf{M}_{33} & \mathsf{M}_{34} & \mathsf{M}_{35} & \mathsf{M}_{36} \\ 0 & 0 & 0 & 0 & 1 & 0 \\ \mathsf{M}_{51} & \mathsf{M}_{52} & 0 & \mathsf{M}_{54} & \mathsf{M}_{55} & \mathsf{M}_{56} \\ \mathsf{M}_{61} & \mathsf{M}_{62} & \mathsf{M}_{63} & \mathsf{M}_{64} & \mathsf{M}_{65} & 0 \end{bmatrix}. \tag{85}$$

The expressions for the elements M_{ij} are fairly lengthy and listed in Appendix B.

The boundary conditions (80)–(82) are correspondingly written

$$\mathbf{B}\mathbf{y} = \mathbf{0} \quad \text{on } r = a, b, \tag{86}$$

with $\mathbf{B} = [\mathsf{B}_{ij}]$, $i \in \{1, 2, 3\}, j \in \{1, \ldots, 6\}$, where

$$\mathbf{B} = \begin{bmatrix} m & 0 & 0 & 1 & -r & 0 \\ \mathsf{B}_{21} & r & r^2 & 0 & 0 & 0 \\ \mathsf{B}_{31} & \mathsf{B}_{32} & 0 & m\mathsf{B}_{31} & 0 & -r \end{bmatrix}, \tag{87}$$

with $\mathsf{B}_{21} = \alpha^2 r^2 + m^2 - 1$ and

$$\mathsf{B}_{31} = \mathcal{A}_{01133} - \mathcal{A}_{02233}, \quad \mathsf{B}_{32} = r(\mathcal{A}_{03333} + \mathcal{A}_{03131} - \mathcal{A}_{01331} - \mathcal{A}_{02233}).$$

5.2 Axisymmetric bifurcations

For axisymmetric bifurcations we take $v = 0$ and u and w to be independent of θ, so that the components of the displacement gradient specialize to

$$[L_{ij}] = \begin{bmatrix} u/r & 0 & 0 \\ 0 & w_z & w_r \\ 0 & u_z & u_r \end{bmatrix}, \tag{88}$$

and the incompressibility condition then has the form

$$u/r + w_z + u_r = 0. \tag{89}$$

For axisymmetric incremental deformations with no dependence on θ and $v = 0$ the component of the equilibrium equation (48) for $i = 1$ is satisfied identically, while the components for $i = 3, 2$ specialize, respectively, to

$$\dot{T}_{023,2} + \dot{T}_{033,3} + (\dot{T}_{033} - \dot{T}_{011})/r = 0, \tag{90}$$

$$\dot{T}_{022,2} + \dot{T}_{032,3} + \dot{T}_{032}/r = 0, \tag{91}$$

wherein the components are given by (62)–(64) and (67). Substitution of these components into (90) and (91) and use of (89) yields

$$\begin{aligned} \dot{p}_z &= \mathcal{A}_{03232} w_{rr} + (r\mathcal{A}'_{03232} + \mathcal{A}_{03232}) w_r/r + \mathcal{A}_{02222} w_{zz} + (\mathcal{A}_{02233} + \mathcal{A}_{03223}) u_{rz} \\ &\quad + (r\mathcal{A}'_{03232} + \mathcal{A}_{03232} - \mathcal{A}_{01212} + \mathcal{A}_{01122} + \mathcal{A}_{01221}) u_z/r, \end{aligned} \tag{92}$$

$$\begin{aligned} \dot{p}_r &= (r\mathcal{A}'_{01133} - \mathcal{A}_{01111}) u/r^2 + (r\mathcal{A}'_{03333} + rp' + \mathcal{A}_{03333}) u_r/r + \mathcal{A}_{03333} u_{rr} \\ &\quad + \mathcal{A}_{02323} u_{zz} + (r\mathcal{A}'_{02233} + \mathcal{A}_{02233} - \mathcal{A}_{01122}) w_z/r + (\mathcal{A}_{02233} + \mathcal{A}_{03223}) w_{rz}. \end{aligned} \tag{93}$$

Alternatively, equations (93) and (92) can be obtained directly from (70) and (69) with $v = 0$, no dependence on θ and use of (89), recalling that p' is given by (71). The traction boundary condition again has the form (72) but now specialized with $i = 2, 3$, yielding again $(73)_2$ and (74).

With $m = 0$ the solutions (75) specialize to

$$u = f(r)\cos\alpha z, \quad w = h(r)\sin\alpha z, \quad \dot{p} = k(r)\cos\alpha z. \tag{94}$$

We cross-differentiate expressions (93) and (92) with respect to z and r, respectively, and eliminate the terms in $\dot{p}$. We also eliminate $h(r)$ from the resulting expression by using incompressibility condition (89). Thus, we obtain the equation for $f(r)$, which depends on α:

$$\begin{aligned} &\mathcal{A}_{03232} r^4 f'''' + 2(r\mathcal{A}'_{03232} + \mathcal{A}_{03232}) r^3 f''' \\ &+ [r^2\mathcal{A}''_{03232} + 3r\mathcal{A}'_{03232} - 3\mathcal{A}_{03232} + \alpha^2 r^2 (2\mathcal{A}_{02233} + 2\mathcal{A}_{03223} - \mathcal{A}_{02222} - \mathcal{A}_{03333})] r^2 f'' \\ &+ [r^2\mathcal{A}''_{03232} - 3r\mathcal{A}'_{03232} + 3\mathcal{A}_{03232} + \alpha^2 r^2 (2r\mathcal{A}'_{03223} + 2r\mathcal{A}'_{02233} - r\mathcal{A}'_{02222} - r\mathcal{A}'_{03333} \\ &\qquad - \mathcal{A}_{02222} - \mathcal{A}_{03333} + 2\mathcal{A}_{02233} + 2\mathcal{A}_{03223})] r f' \\ &+ [-r^2\mathcal{A}''_{03232} + 3r\mathcal{A}'_{03232} - 3\mathcal{A}_{03232} + \alpha^2 r^2 (r^2\mathcal{A}''_{03223} + r^2 p'' + r\mathcal{A}'_{03223} + r\mathcal{A}'_{01122} \\ &\qquad - r\mathcal{A}'_{01133} - r\mathcal{A}'_{02222} + r\mathcal{A}'_{02233} + \mathcal{A}_{01111} + \mathcal{A}_{02222} - 2\mathcal{A}_{01122} - 2\mathcal{A}_{03223})] f \\ &+ \alpha^4 r^4 \mathcal{A}_{02323} f. \end{aligned} \tag{95}$$

Note that from (71) we obtain

$$r^2 p'' = r^2 \mathcal{A}''_{03131} - r^2 \mathcal{A}''_{03113} + r\mathcal{A}'_{03131} - r\mathcal{A}'_{01313} - \mathcal{A}_{03131} + \mathcal{A}_{01313}. \tag{96}$$

In terms of f the corresponding boundary conditions $(73)_2$ and (74) become

$$r^2 f'' + rf' + (\alpha^2 r^2 - 1)f = 0 \quad \text{on } r = a, b \tag{97}$$

and

$$\begin{aligned}
&\mathcal{A}_{03232} r^3 f''' + (r\mathcal{A}'_{03232} + 2\mathcal{A}_{03232}) r^2 f'' \\
&+ [r\mathcal{A}'_{03232} - \mathcal{A}_{03232} - \alpha^2 r^2 (\mathcal{A}_{03333} + \mathcal{A}_{02222} - 2\mathcal{A}_{02233} - 2\mathcal{A}_{03223} + \mathcal{A}_{03232})] r f' \\
&+ [-r\mathcal{A}'_{03232} + \mathcal{A}_{03232} + \alpha^2 r^2 (r\mathcal{A}'_{03232} + \mathcal{A}_{01122} - \mathcal{A}_{02222} + \mathcal{A}_{02233} - \mathcal{A}_{01133} \\
&\qquad + \mathcal{A}_{03232} + \mathcal{A}_{01221} - \mathcal{A}_{01212})] f = 0 \quad \text{on } r = a, b.
\end{aligned} \tag{98}$$

As with the asymmetric case, we arrange a first-order system with $\mathbf{y} = (y_1, y_2, y_3, y_4)$ with four instead of six variables, now defined by

$$y_1 = f, \quad y_2 = y_1' = f', \quad y_3 = y_2' = f'', \quad y_4 = y_3' = f'''. \tag{99}$$

Thus, $\mathbf{y}' = \mathsf{M}\mathbf{y}$, where, instead of (85),

$$\mathsf{M} = \begin{bmatrix} 0 & 1 & 0 & 0 \\ 0 & 0 & 1 & 0 \\ 0 & 0 & 0 & 1 \\ \mathsf{M}_{41} & \mathsf{M}_{42} & \mathsf{M}_{43} & \mathsf{M}_{44} \end{bmatrix}. \tag{100}$$

The elements M_{4i}, $i \in \{1, 2, 3, 4\}$, are listed in Appendix B.

The boundary conditions are again written as in (86), but now with B as the 2×4 matrix

$$\mathsf{B} = \begin{bmatrix} \mathsf{B}_{11} & r & r^2 & 0 \\ \mathsf{B}_{21} & \mathsf{B}_{22} & \mathsf{B}_{23} & \mathsf{B}_{24} \end{bmatrix}, \tag{101}$$

where $\mathsf{B}_{11} = \alpha^2 r^2 - 1$,

$$\begin{aligned}
\mathsf{B}_{21} &= -r\mathcal{A}'_{03232} + \mathcal{A}_{03232} + \alpha^2 r^2 (r\mathcal{A}'_{03232} + \mathcal{A}_{01122} - \mathcal{A}_{02222} + \mathcal{A}_{02233} - \mathcal{A}_{01133} \\
&\qquad + \mathcal{A}_{03232} + \mathcal{A}_{01221} - \mathcal{A}_{01212}), \\
\mathsf{B}_{22} &= [r\mathcal{A}'_{03232} - \mathcal{A}_{03232} - \alpha^2 r^2 (\mathcal{A}_{03333} + \mathcal{A}_{02222} - 2\mathcal{A}_{02233} - 2\mathcal{A}_{03223} + \mathcal{A}_{03232})] r, \\
\mathsf{B}_{23} &= (r\mathcal{A}'_{03232} + 2\mathcal{A}_{03232}) r^2, \quad \mathsf{B}_{24} = \mathcal{A}_{03232} r^3.
\end{aligned} \tag{102}$$

5.3 Prismatic bifurcations

For prismatic bifurcations u, v and w are independent of z. Furthermore, the equation for w decouples from those for u and v and any solution for w does not affect the cross-sectional shape of the tube. It is therefore convenient to set $w = 0$. The matrix of components of $\mathbf{L}$ then specializes to

$$[L_{ij}] = \begin{bmatrix} (u + v_\theta)/r & 0 & v_r \\ 0 & 0 & 0 \\ (u_\theta - v)/r & 0 & u_r \end{bmatrix}, \tag{103}$$

and the incompressibility condition reduces to

$$u + v_\theta + r u_r = 0. \tag{104}$$

First, we note that the equilibrium equation for $i = 2$ in (48) is satisfied identically, while the equations for $i = 1, 3$ yield

$$\dot{T}_{011,1} + \dot{T}_{031,3} + (\dot{T}_{031} + \dot{T}_{013})/r = 0, \tag{105}$$

$$\dot{T}_{013,1} + \dot{T}_{033,3} + (\dot{T}_{033} - \dot{T}_{011})/r = 0. \tag{106}$$

For the considered underlying cylindrical configuration the components of $\dot{\mathbf{T}}_0$ in the above two equations are given by (62), (64) and (66). Then, by substitution of these expressions into (105) and (106) and use of the incompressibility condition (104), we obtain

$$\begin{aligned}\dot{p}_\theta &= [r(\mathcal{A}'_{03113} + p') + \mathcal{A}_{01313}](u_\theta - v)/r + (r\mathcal{A}'_{03131} + \mathcal{A}_{03131})v_r + \mathcal{A}_{03131} r v_{rr} \\ &\quad + (\mathcal{A}_{01331} + \mathcal{A}_{01133} - \mathcal{A}_{01111})u_{r\theta}, \end{aligned} \tag{107}$$

$$\begin{aligned}\dot{p}_r &= [r(\mathcal{A}'_{03333} + p' - \mathcal{A}'_{01133}) + \mathcal{A}_{03333} + \mathcal{A}_{01111} - 2\mathcal{A}_{01133}]u_r/r \\ &\quad + (\mathcal{A}_{03333} - \mathcal{A}_{01133})u_{rr} + \mathcal{A}_{01313}(u_{\theta\theta} - v_\theta)/r^2 + \mathcal{A}_{01331} v_{r\theta}/r, \end{aligned} \tag{108}$$

where p' is again given by (71).

We now write the solutions in the form

$$u = f(r)\cos m\theta, \quad v = g(r)\sin m\theta, \quad \dot{p} = k(r)\cos m\theta, \tag{109}$$

corresponding to $\alpha = 0$ in (75).

Thus, from the incompressibility condition (104) we obtain

$$r f'(r) + f(r) + m g(r) = 0. \tag{110}$$

We substitute expressions (109) into (107) and (108) and, by cross differentiation to eliminate $\dot{p}$ and use of (110), we obtain an equation for $f(r)$, which depends on m:

$$\begin{aligned}&\mathcal{A}_{03131} r^4 f'''' + 2(r\mathcal{A}'_{03131} + 3\mathcal{A}_{03131})r^3 f''' + [r^2\mathcal{A}''_{03131} + 7r\mathcal{A}'_{03131} + 5\mathcal{A}_{03131} \\ &+ m^2(2\mathcal{A}_{01133} + 2\mathcal{A}_{01331} - \mathcal{A}_{01111} - \mathcal{A}_{03333})]r^2 f'' \\ &+ [r^2\mathcal{A}''_{03131} + m^2 r(2\mathcal{A}'_{01133} + 2\mathcal{A}'_{01331} - \mathcal{A}'_{01111} - \mathcal{A}'_{03333}) \\ &+ r\mathcal{A}'_{03131} - \mathcal{A}_{03131} + m^2(2\mathcal{A}_{01133} + 2\mathcal{A}_{01331} - \mathcal{A}_{01111} - \mathcal{A}_{03333})]r f' \\ &+ (m^2 - 1)(r^2\mathcal{A}''_{03131} + r\mathcal{A}'_{03131} - \mathcal{A}_{03131} + m^2\mathcal{A}_{01313})f = 0. \end{aligned} \tag{111}$$

The relevant boundary conditions in this case are (72) with $i = 1, 3$. First, the boundary condition $(73)_1$ yields

$$r(L_{13} + L_{31}) \equiv r v_r + u_\theta - v = 0 \quad \text{on } r = a, b, \tag{112}$$

while on use of $L_{11} + L_{33} = 0$ with $L_{22} = 0$ the boundary condition (74) specializes to

$$(\mathcal{A}_{03333} - \mathcal{A}_{03311} + \mathcal{A}_{03131} - \mathcal{A}_{03113})L_{33} - \dot{p} = 0 \quad \text{on } r = a, b, \tag{113}$$

with $L_{33} = u_r$. The term in $\dot{p}$ is eliminated by differentiating (113) with respect to θ and using (107).

On use of the incompressibility condition (110), (107) to eliminate $k(r)$, and (54), the boundary conditions (112) and (113) are rewritten in terms of f as

$$r^2 f'' + r f' + (m^2 - 1) f = 0 \quad \text{on } r = a, b, \tag{114}$$

$$\begin{aligned}
&\mathcal{A}_{03131} r^3 f''' + (r\mathcal{A}'_{03131} + 4\mathcal{A}_{03131}) r^2 f'' \\
&+ [r\mathcal{A}'_{03131} + \mathcal{A}_{03131} + m^2(2\mathcal{A}_{01331} + 2\mathcal{A}_{01133} - \mathcal{A}_{01111} - \mathcal{A}_{03333} - \mathcal{A}_{03131})] r f' \\
&+ (m^2 - 1)(r\mathcal{A}'_{03131} + \mathcal{A}_{03131}) f = 0 \quad \text{on } r = a, b.
\end{aligned} \tag{115}$$

As a first-order system we again use the definition in (99)–(100), with the components M_{4i} listed in Appendix B. The corresponding boundary matrix is again given by (101), but in this case with $\mathsf{B}_{11} = m^2 - 1$,

$$\begin{aligned}
&\mathsf{B}_{21} = (m^2 - 1)(r\mathcal{A}'_{03131} + \mathcal{A}_{03131}), \\
&\mathsf{B}_{22} = [r\mathcal{A}'_{03131} + \mathcal{A}_{03131} + m^2(2\mathcal{A}_{01331} + 2\mathcal{A}_{01133} - \mathcal{A}_{01111} - \mathcal{A}_{03333} - \mathcal{A}_{03131})] r, \\
&\mathsf{B}_{23} = (r\mathcal{A}'_{03131} + 4\mathcal{A}_{03131}) r^2, \quad \mathsf{B}_{24} = \mathcal{A}_{03131} r^3.
\end{aligned} \tag{116}$$

5.4 Non-dimensionalization

The asymmetric and axisymmetric problems require boundary conditions on the ends of the tube. For this purpose we assume that there is no incremental axial displacement, i.e $w = 0$, and no incremental shear stress, i.e. $\dot{T}_{023} = 0$ and $\dot{T}_{021} = 0$ on the ends $z = 0, l$. Since, from (75), $(65)_2$, $(67)_1$ and (57), each of these is proportional to $\sin \alpha z$, it follows that

$$\alpha = \frac{\pi n}{l} = \frac{\pi n}{\lambda_z L}, \tag{117}$$

where $n = 1, 2, 3, ...$ is the mode number. Clearly, since a change in n is equivalent to a change in L it is convenient to fix $n = 1$, noting that an increase in the mode number n is captured by a decrease in the value of L.

We use the dimensionless variables and material constants defined by

$$\begin{aligned}
&\bar{R} = R/A, \quad \bar{B} = B/A, \quad \bar{L} = L/A, \quad \bar{r} = r/A, \quad \bar{a} = a/A, \quad \bar{b} = b/A, \\
&\bar{\alpha} = \alpha A, \quad \bar{\nu} = \nu A^2/\mu, \quad \bar{\kappa} = \kappa\mu, \quad \bar{\boldsymbol{\tau}} = \boldsymbol{\tau}/\mu, \quad \bar{\boldsymbol{\mathcal{A}}}_0 = \boldsymbol{\mathcal{A}}_0/\mu,
\end{aligned} \tag{118}$$

where, from (41) and (42), the components of $\bar{\boldsymbol{\tau}}$ are functions of $\bar{R}$, while the components of $\bar{\boldsymbol{\mathcal{A}}}_0$ are functions of $\bar{r}$.

We also introduce non-dimensional variables

$$\bar{f}(\bar{r}) = f(r)/A, \quad \bar{g}(\bar{r}) = g(r)/A, \quad \bar{p}(\bar{r}) = p(r)/\mu, \quad \bar{k}(\bar{r}) = k(r)/\mu. \tag{119}$$

For the asymmetric problem we then define the components of $\bar{\mathbf{y}}$ by

$$\begin{aligned}
&\bar{y}_1(\bar{r}) = \bar{f}(\bar{r}), \quad \bar{y}_2(\bar{r}) = \bar{f}'(\bar{r}), \quad \bar{y}_3(\bar{r}) = \bar{f}''(\bar{r}), \\
&\bar{y}_4(\bar{r}) = \bar{g}(\bar{r}), \quad \bar{y}_5(\bar{r}) = \bar{g}'(\bar{r}), \quad \bar{y}_6(\bar{r}) = \bar{k}(\bar{r}),
\end{aligned} \tag{120}$$

where a prime now stands for differentiation with respect to $\bar{r}$.

With the notation $\bar{\mathbf{y}} = (\bar{y}_1, \bar{y}_2, \bar{y}_3, \bar{y}_4, \bar{y}_5, \bar{y}_6)$, the first-order system can then be written in the dimensionless form

$$\bar{\mathbf{y}}' = \bar{\mathbf{M}}\bar{\mathbf{y}}, \tag{121}$$

where

$$\bar{y}_1 = y_1/A, \quad \bar{y}_2 = y_2, \quad \bar{y}_3 = Ay_3, \quad \bar{y}_4 = y_4/A, \quad \bar{y}_5 = y_5, \quad \bar{y}_6 = y_6/\mu, \tag{122}$$

and the dimensionless forms $\bar{\mathsf{M}}_{ij}$ of the components M_{ij} are given by

$$\begin{gathered}
\bar{\mathsf{M}}_{31} = \mathsf{M}_{31}A^3, \quad \bar{\mathsf{M}}_{32} = \mathsf{M}_{32}A^2, \quad \bar{\mathsf{M}}_{33} = \mathsf{M}_{33}A, \quad \bar{\mathsf{M}}_{34} = \mathsf{M}_{34}A^3, \\
\bar{\mathsf{M}}_{35} = \mathsf{M}_{35}A^2, \quad \bar{\mathsf{M}}_{36} = \mu\mathsf{M}_{36}A^2, \\
\bar{\mathsf{M}}_{51} = \mathsf{M}_{51}A^2, \quad \bar{\mathsf{M}}_{52} = \mathsf{M}_{52}A, \quad \bar{\mathsf{M}}_{54} = \mathsf{M}_{54}A^2, \quad \bar{\mathsf{M}}_{55} = \mathsf{M}_{55}A, \quad \bar{\mathsf{M}}_{56} = \mu\mathsf{M}_{66}A, \\
\bar{\mathsf{M}}_{61} = \mathsf{M}_{61}A^2/\mu, \ \bar{\mathsf{M}}_{62} = \mathsf{M}_{62}A/\mu, \ \bar{\mathsf{M}}_{63} = \mathsf{M}_{63}/\mu, \ \bar{\mathsf{M}} = \mathsf{M}_{64}A^2/\mu, \ \bar{\mathsf{M}}_{65} = \mathsf{M}_{65}A/\mu,
\end{gathered}$$

recalling that $\mathsf{M}_{53} = \mathsf{M}_{66} = 0$.

The corresponding boundary condition is

$$\bar{\mathbf{B}}\bar{\mathbf{y}} = \mathbf{0} \quad \text{on } \bar{r} = \bar{a}, \bar{b}, \tag{123}$$

where

$$\bar{\mathbf{B}} = \begin{bmatrix} m & 0 & 0 & 1 & -\bar{r} & 0 \\ \mathsf{B}_{21} & \bar{r} & \bar{r}^2 & 0 & 0 & 0 \\ \bar{\mathsf{B}}_{31} & \bar{\mathsf{B}}_{32} & 0 & m\bar{\mathsf{B}}_{31} & 0 & -\bar{r} \end{bmatrix}, \tag{124}$$

with $\bar{\mathsf{B}}_{31} = \mathsf{B}_{31}/\mu$, $\bar{\mathsf{B}}_{32} = \mathsf{B}_{32}/(\mu A)$.

For the axisymmetric case, we have

$$\begin{gathered}
\bar{y}_1 = y_1/A, \quad \bar{y}_2 = y_2, \quad \bar{y}_3 = Ay_3, \quad \bar{y}_4 = A^2y_4, \\
\bar{\mathsf{M}}_{41} = A^4\mathsf{M}_{41}, \quad \bar{\mathsf{M}}_{42} = A^3\mathsf{M}_{42}, \quad \bar{\mathsf{M}}_{43} = A^2\mathsf{M}_{43}, \quad \bar{\mathsf{M}}_{44} = A\mathsf{M}_{41},
\end{gathered}$$

and

$$\bar{\mathbf{B}} = \begin{bmatrix} \mathsf{B}_{11} & \bar{r} & \bar{r}^2 & 0 \\ \bar{\mathsf{B}}_{21} & \bar{\mathsf{B}}_{22} & \bar{\mathsf{B}}_{23} & \bar{\mathsf{B}}_{24} \end{bmatrix}, \tag{125}$$

with $\bar{\mathsf{B}}_{21} = \mathsf{B}_{21}/\mu$, $\bar{\mathsf{B}}_{22} = \mathsf{B}_{22}/(\mu A)$, $\bar{\mathsf{B}}_{23} = \mathsf{B}_{23}/(\mu A^2)$, $\bar{\mathsf{B}}_{24} = \mathsf{B}_{24}/(\mu A^3)$.

For the prismatic case the equation and boundary condition have the same structure as for the axisymmetric case, but the values of the M_{4i} (see Appendix B), B_{11} and B_{2i}, $i \in \{1, 2, 3, 4\}$ are different.

6 Numerical results

Solutions of the systems are obtained using the routine `NDSolve` in Mathematica (2020). Firstly, results are obtained for the axisymmetric case, followed by the prismatic case and finally the asymmetric case. The results are presented as bifurcation curves in the (λ_z, λ_a) plane, where $\lambda_a = a/A$ (the value of λ_θ on the inner boundary $r = a$), for different values of the geometric parameters $\bar{B} = B/A$, $\bar{L} = L/A$, the material parameter $\bar{\kappa}$ and the

residual stress parameter $\bar{\nu}$. Also included in each case are plots of the equation $P = 0$, which is independent of $\bar{\nu}$ for the case $\bar{\kappa} = 0$ but dependent on $\bar{\nu}$ for $\bar{\kappa} \neq 0$.

In Dorfmann and Ogden (2021) details of the restrictions imposed by the strong ellipticity condition on the deformation for a residually stressed tube for the considered strain-energy function were provided. In particular, these limit the range of allowable values of the parameter quantifying the magnitude of the residual stress, and are therefore accounted for in the following illustrations.

6.1 Axisymmetric results

The numerical results for the axisymmetric case are based on the equations given in Section 5.2. We begin with Figs. 1 and 2 in which λ_a is plotted against λ_z for $\bar{B} = 1.2$ and three different values of $\bar{L}$ in each case. The plots in Fig. 1 are for the reduced model (36) with $\bar{\kappa} = 0$ and with (a) $\bar{\nu} = 0$ (no residual stress) and (b) $\bar{\nu} = 5$ (showing the changes due to residual stress). Plots for $\bar{\nu} = -5$ are not shown separately since they are almost identical to those for $\bar{\nu} = 5$. Points on the curves correspond to values of (λ_z, λ_a) at which bifurcation is possible, for example for changes in λ_a due to internal or external pressure when λ_z is fixed. Reduction of $\bar{L}$ reduces or increases the value of λ_a at which bifurcation becomes possible depending on the value of λ_z. We recall from Section 5.4 that n has been taken as 1, so that a reduction in the value of $\bar{L}$ or $\lambda_z\bar{L}$ corresponds to an increase in the mode number. The results in Fig. 1(a) are consistent with those for a different strain-energy function obtained by Haughton and Ogden (1979b), who restricted attention to the positive pressure region.

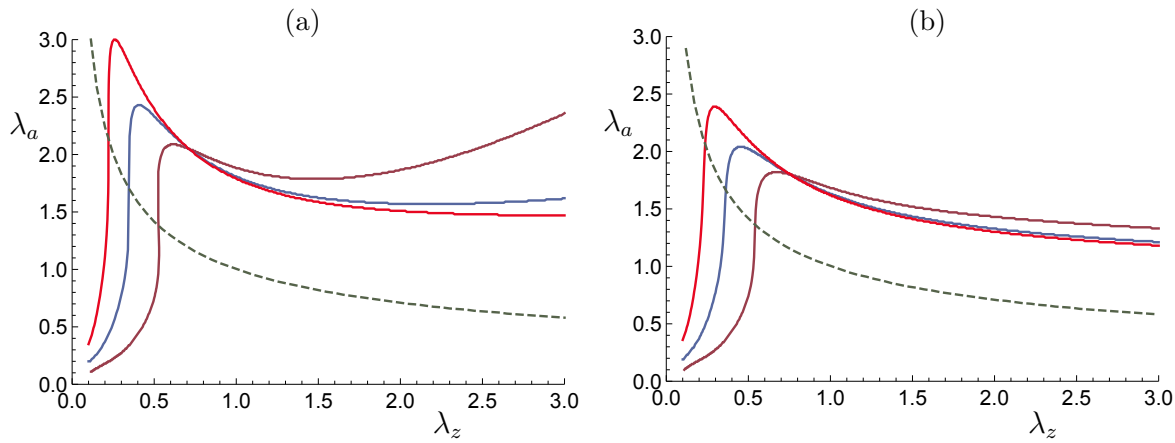

Figure 1: Plots of the axisymmetric bifurcation curves in (λ_z, λ_a) space for the model (36) for $\bar{\kappa} = 0$ with $\bar{B} = 1.2$, $\bar{L} = 5$ (purple), 10 (blue), 20 (red): (a) $\bar{\nu} = 0$; (b) $\bar{\nu} = 5$. The dashed curves correspond to zero pressure.

Also shown in each figure is the (dashed) curve corresponding to zero pressure ($P = 0$), which is independent of $\bar{\nu}$ for $\bar{\kappa} = 0$. Above (below) this curve the effective pressure $P = P_a - P_b$ is internal (external).

The effect of a change in the value of the material parameter $\bar{\kappa}$ is illustrated in Fig. 2 for $\bar{\kappa} = 1$. The curves for $\bar{\nu} = 0$ are the same as in Fig. 1(a). Figures 2(a) and (b), respectively, are for $\bar{\nu} = 5$ and $\bar{\nu} = -5$, and show that there is a slight difference between

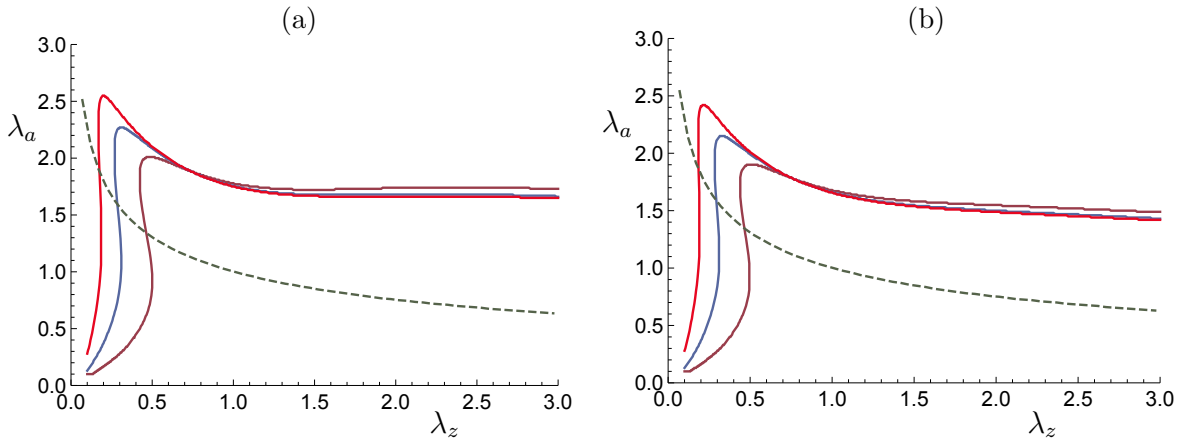

Figure 2: Plots of the axisymmetric bifurcation curves in (λ_z, λ_a) space for the model (36) for $\bar{\kappa} = 1$ with $\bar{B} = 1.2$, $\bar{L} = 5$ (purple), 10 (blue), 20 (red): (a) $\bar{\nu} = 5$; (b) $\bar{\nu} = -5$. The dashed curves correspond to zero pressure. See Fig. 1(a) for the case $\bar{\nu} = 0$.

the results for these two values. In general, the zero pressure curves depend on $\bar{\nu}$, but they are not distinguishable in this case. For $\bar{\nu} = 5$, comparison of Fig. 2(a) with Fig. 1(b) shows that in general the value of λ_a is larger for latter.

Figures 3 and 4 present the results of Figs. 1 and 2 from a different perspective, for two values of $\bar{L}$ separately and with different values of $\bar{\nu}$ in each case, with the addition of curves for $\bar{\nu} = \pm 10$. With $\bar{\kappa} = 0$, Figs. 3(a), (b) are for $\bar{L} = 5, 20$, respectively. The curves for $\bar{\nu} = \pm 5$ are very similar, as is also the case for $\bar{\nu} = \pm 10$, and the general trend that the value of λ_a at bifurcation for fixed values of λ_z is reduced by the presence of residual stress can be seen. The curves for $\bar{\nu} = \pm 10$ in Fig. 3 lie outside the region where strong ellipticity holds in this case.

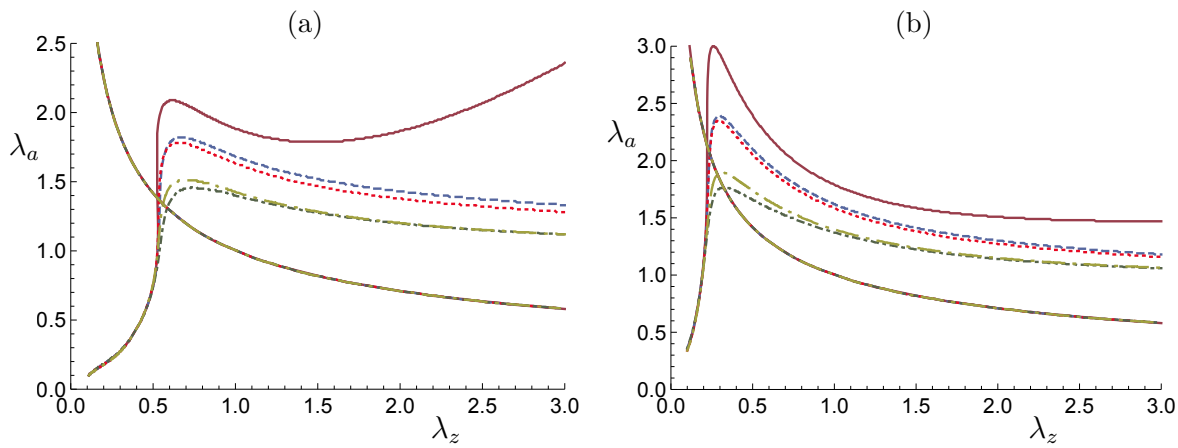

Figure 3: Plots of the axisymmetric bifurcation curves in (λ_z, λ_a) space for the model (36) for $\bar{\kappa} = 0$ with $\bar{B} = 1.2$: (a) $\bar{L} = 5$, (b) $\bar{L} = 20$. In each case, curves are shown for $\bar{\nu} = -10$ (yellow dash-dot), -5 (red dots), 0 (purple continuous), 5 (blue dashes), 10 (green dash-dot). The coincident (dashed) zero pressure curves are independent of $\bar{\nu}$.

Figure 4 shows the corresponding results for $\bar{\kappa} = 1$. In this case the zero pressure

curve is dependent on the value of $\bar{\nu}$. Note, in particular, that the curves for $\bar{\nu} = \pm 10$ fall outside the region for which the strong ellipticity condition identified in Dorfmann and Ogden (2021) holds if λ_a is less than approximately 1.1 when λ_z is less than 1.

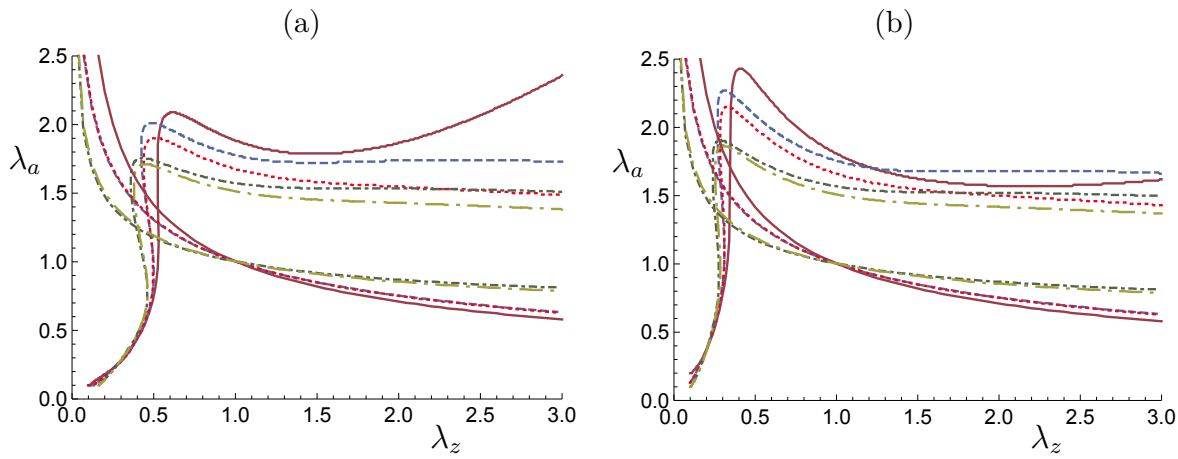

Figure 4: Plots of the axisymmetric bifurcation curves in (λ_z, λ_a) space for the model (36) for $\bar{\kappa} = 1$ with $\bar{B} = 1.2$: (a) $\bar{L} = 5$, (b) $\bar{L} = 20$. In each case, curves are shown for $\bar{\nu} = -10$ (yellow dash-dot), -5 (red dots), 0 (purple continuous), 5 (blue dashes), 10 (green dash-dot). The zero pressure curves, which coincide for $\lambda_a = \lambda_z = 1$, are dependent on $\bar{\nu}$, very nearly independent of the sign of $\bar{\nu}$, and colour coded with the corresponding bifurcation curves.

Figure 5 illustrates the regions of strong ellipticity in $(\lambda_a, \bar{\nu})$ space for $\bar{\kappa} = 1$, $\bar{B} = 1.2$ and fixed $\lambda_z = 0.8, 1, 1.2$ as a backdrop for the figures here and in subsequent subsections. Note, in particular, that the strongly elliptic region moves to the left as λ_z increases.

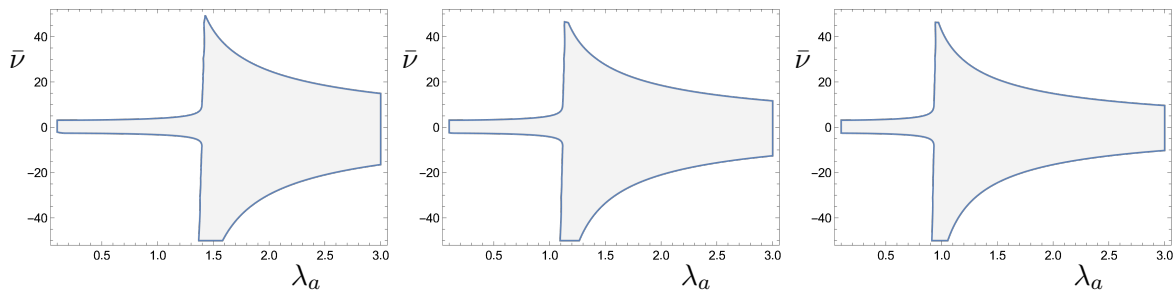

Figure 5: Regions for which strong ellipticity holds (shaded) in plots of $\bar{\nu}$ versus λ_a for $\bar{B} = 1.2$ and $\bar{\kappa} = 1$: left to right: $\lambda_z = 0.8, 1, 1.2$.

Detailed calculations parallel to those illustrated above have been carried out for thicker walled tubes, and their general characters are very similar to those in Figs. 1–4. Thus, these results are not included here. The situation in this regard is somewhat different in the case of prismatic bifurcations, as will be seen in the following subsection.

6.2 Prismatic results

Some results for prismatic bifurcations were given in Dorfmann and Ogden (2021) in the form of $\bar{\nu}$ versus $\bar{a} = \lambda_a$ for the case $\lambda_z = 1$ for $\bar{\kappa} = 0, 0.5$ and $\bar{B} = 1.1, 1.2, 1.5$ for a wide range of mode numbers. Here we provide a limited number of additional results but in the form of λ_a versus λ_z for $\bar{\kappa} = 0, 1$ and $\bar{\nu} = 0, 5, 10$ with a small selection of mode numbers m for illustration based on the equations in Section 5.3.

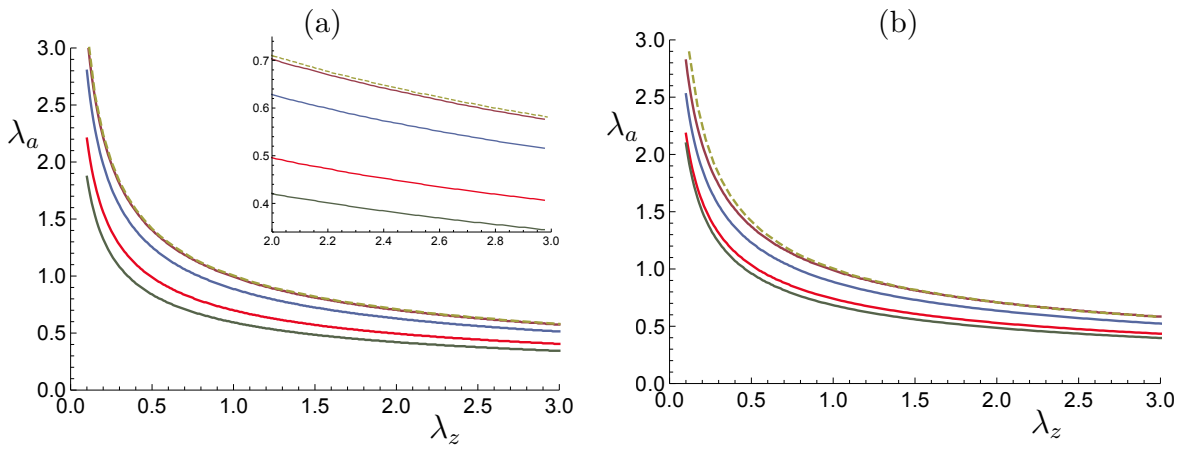

Figure 6: Prismatic bifurcation curves for $\bar{B} = 1.2$, with $\bar{\kappa} = 0$ for mode numbers $m = 2$ (purple), $m = 6$ (blue), $m = 10$ (red), $m = 14$ (green): (a) $\bar{\nu} = 0$, (b) $\bar{\nu} = 5$. The zero pressure curve is represented by the dashed curve. The zoom inset in (a) shows that the $m = 2$ curve is below the zero pressure curve.

First, Fig. 6 is for $\bar{\kappa} = 0$ with $\bar{B} = 1.2$ and $\bar{\nu} = 0, 5$ in (a) and (b), respectively, with bifurcation curves shown for mode numbers $m = 2, 6, 10, 14$ along with the zero pressure curve. The latter is almost indistinguishable from the $m = 2$ bifurcation curve in (a) so a zoom of part of the region is shown in the inset to show that the $m = 2$ bifurcation curve is below the zero pressure curve, i.e. in the region of external pressure, and this is also the case for the parts of the curves not shown in the inset. Clearly, the general character of the results is only slightly modified by the change from $\bar{\nu} = 0$ to $\bar{\nu} = 5$. The results in (a) are for the case without residual stress, which was examined in Haughton and Ogden (1979b), where, for a different strain-energy function, it was found that the $m = 2$ mode arises first during compression, as is also the situation here. Note that there is no mode $m = 1$ prismatic bifurcation (Haughton and Ogden, 1979b). See also the references in the latter paper.

Figure 7 shows corresponding results for a thicker walled tube with $\bar{B} = 1.4$. In Fig. 7(a) note that the $m = 10$ (red) and $m = 14$ (green) curves are indistinguishable. In the case of Fig. 7(b) the $m = 2$ and $m = 10$ bifurcation curves cross over in the region of high compression, and there are duplicate $m = 14$ bifurcation curves above the zero pressure curve. Thus, bifurcation becomes possible under internal pressure for mode number $m = 14$ as the lower of the two green branches is reached during inflation.

For the same mode numbers as in Fig. 7, Figs. 8 and 9 with $\bar{\nu} = 5$ and $\bar{\nu} = 10$, respectively, compare results for $\bar{B} = 1.2$ and $\bar{B} = 1.4$ with $\bar{\kappa} = 1$. The results for $\bar{\nu} = 0$ with $\bar{B} = 1.2$ are the same as in Fig. 6(a). We refer to Dorfmann and Ogden (2021)

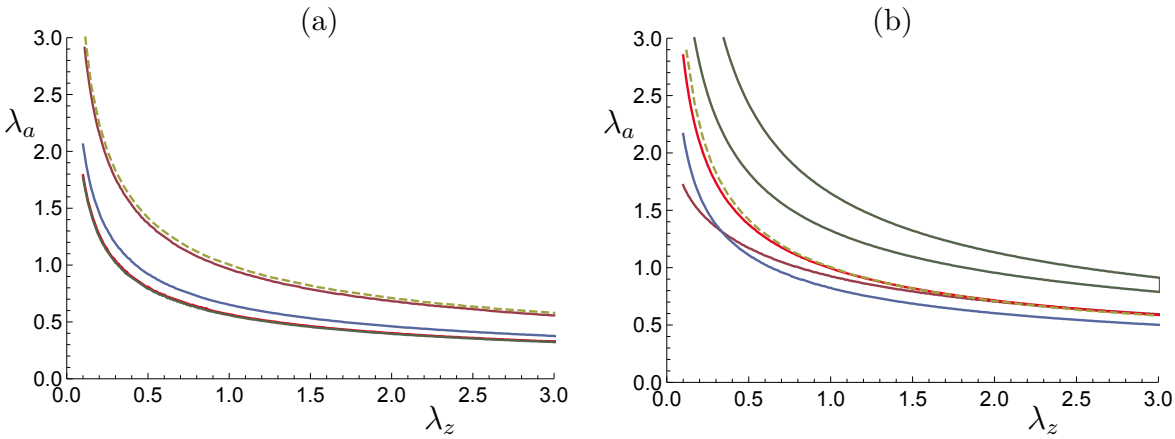

Figure 7: Prismatic bifurcation curves for $\bar{B} = 1.4$, with $\bar{\kappa} = 0$ for mode numbers $m = 2$ (purple), $m = 6$ (blue), $m = 10$ (red), $m = 14$ (green): (a) $\bar{\nu} = 0$, (b) $\bar{\nu} = 5$. The zero pressure curve is represented by the dashed curve. Note that in (a) the $m = 10$ and $m = 14$ curves are indistinguishable.

for results for a wider range of mode numbers and negative values of $\bar{\nu}$ when $\lambda_z = 1$, noting that the results are broadly similar for other values of λ_z except for large axial compression of the tube (λ_z less than approximately 0.5).

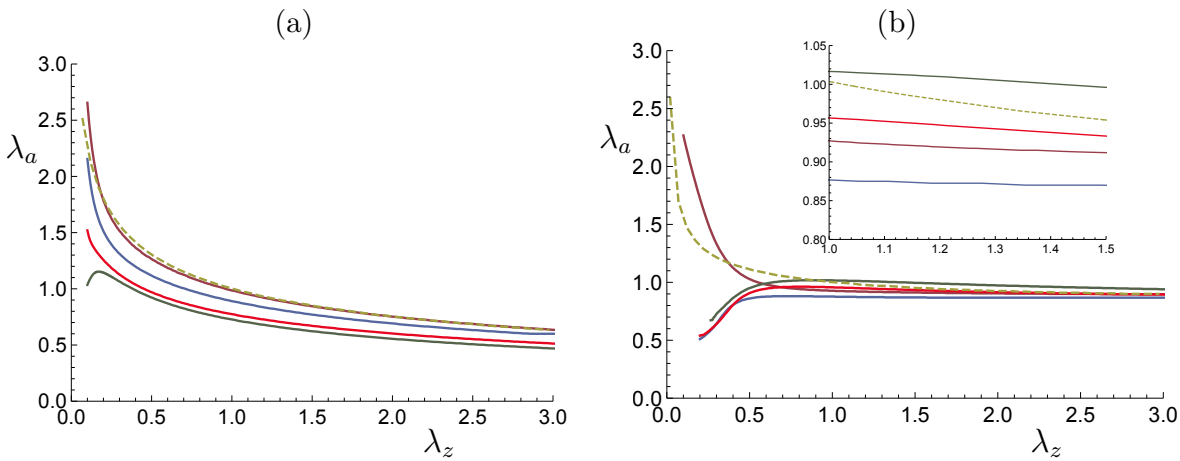

Figure 8: Prismatic bifurcation curves for $\bar{\nu} = 5$, with $\bar{\kappa} = 1$ for mode numbers $m = 2$ (purple), $m = 6$ (blue), $m = 10$ (red), $m = 14$ (green): (a) $\bar{B} = 1.2$, (b) $\bar{B} = 1.4$. The zero pressure curve is represented by the dashed curve.

In Fig. 8(a) the $m = 2$ mode curve crosses into the region of positive pressure under high axial compression, and this is also the case in Fig. 9(a), where the $m = 2$ curve is joined by the $m = 6$ curve in the positive pressure domain for very high axial compression. The other modes remain in the region of negative pressure. In Fig. 9(a), in particular, the curves are close to the $P = 0$ curve except for significant axial compression. This is also the case in Fig. 8(b), where the $m = 2$ curve again crosses from the negative to the positive pressure region as axial compression reaches a significant value, while the $m = 14$ crosses from the negative to positive pressure region as the axial stretch increases, but it

remains only slightly above the zero pressure curve. The $m = 6$ and $m = 10$ curves are below and close to the zero pressure curve except for large axial compression. Thus, for $\lambda_z = 1.3$, for example, the $m = 14$ mode can occur under a slight internal pressure and the $m = 10$ mode is the first to arise under external pressure, followed by the $m = 2$ and then the $m = 6$ modes. A zoom of the region around $\lambda_z = 1.3$ is shown in Fig. 8(b).

In Fig. 9(b) the situation is similar for the $m = 2$ mode, but in this case the $m = 10$ mode crosses slightly into the positive pressure region for λ_z greater than about 0.6. The three modes remain close to the zero pressure curve for λ_z greater than about 0.7. By contrast, there are duplicate $m = 14$ modes significantly below the zero pressure curve, but only for λ_z greater than about 1. There are additional $m = 6$ and $m = 10$ branches in this region, but either the $m = 2$ or $m = 6$ mode becomes possible first under external pressure, depending on the value of λ_z.

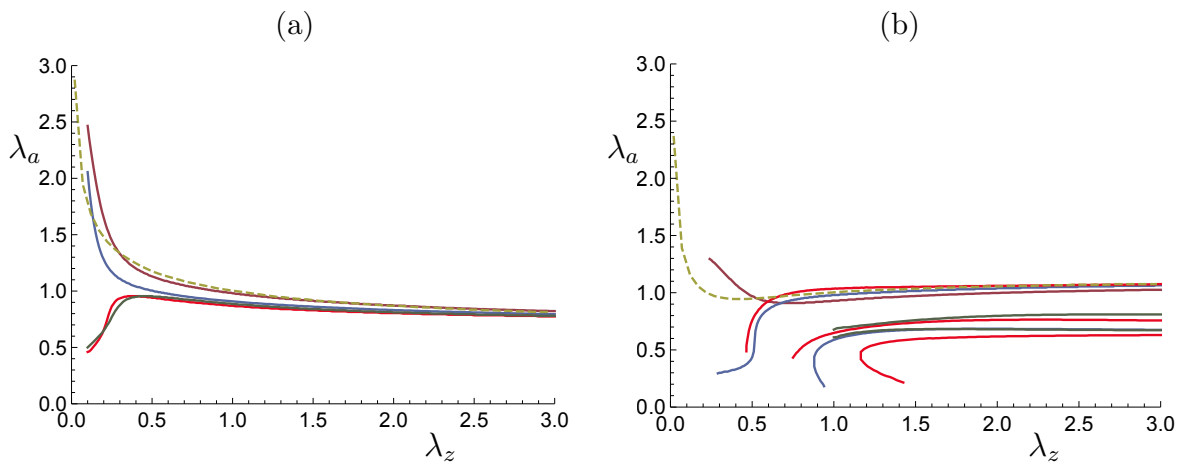

Figure 9: Prismatic bifurcation curves for $\bar{\nu} = 10$, with $\bar{\kappa} = 1$ for mode numbers $m = 2$ (purple), $m = 6$ (blue), $m = 10$ (red), $m = 14$ (green): (a) $\bar{B} = 1.2$, (b) $\bar{B} = 1.4$. The zero pressure curve is represented by the dashed curve.

The above illustrations demonstrate the range of possible bifurcation onset and priorities for a limited number of mode numbers. Other mode numbers can add refinement to these discussions but they don't affect the overall picture. Note, with reference to Fig. 5, the possible values of $\bar{\nu}$ that lie within in strongly elliptic domain, dependent on the value of λ_z, in particular the values of λ_z for which $\bar{\nu} = 5, 10$ are in the strongly elliptic domain for $\bar{\kappa} = 1$.

6.3 Asymmetric results

The equations in Section 5.1 provide the basis for the illustrations in this subsection. We have found that the results do not depend significantly on $\bar{L}$ for its considered range between 5 and 20. Thus, we only show results for the intermediate value $\bar{L} = 10$ in the following figures. The first asymmetric bifurcation results are shown in Fig. 10 for $\bar{B} = 1.2$, $\bar{\kappa} = 0$ and mode numbers $m = 1, 2, 6, 10$. Figure 10(a) is for $\bar{\nu} = 0$, i.e. for the case with no residual stress, for which, in Haughton and Ogden (1979b), asymmetric bifurcation curves were provided for the case $m = 1$, but for a different strain-energy

function. Unlike for the present model, no modes were found for $m \geq 2$ in Haughton and Ogden (1979b). Figure 10(b) is for $\bar{\nu} = 5$, for which the results are essentially identical to those for $\bar{\nu} = 0$.

While for $m = 1$ bifurcation is possible under either internal or external pressure, with increasing m the curves move mainly to the external pressure region (below the zero pressure curve), and more so as m increases further (not shown).

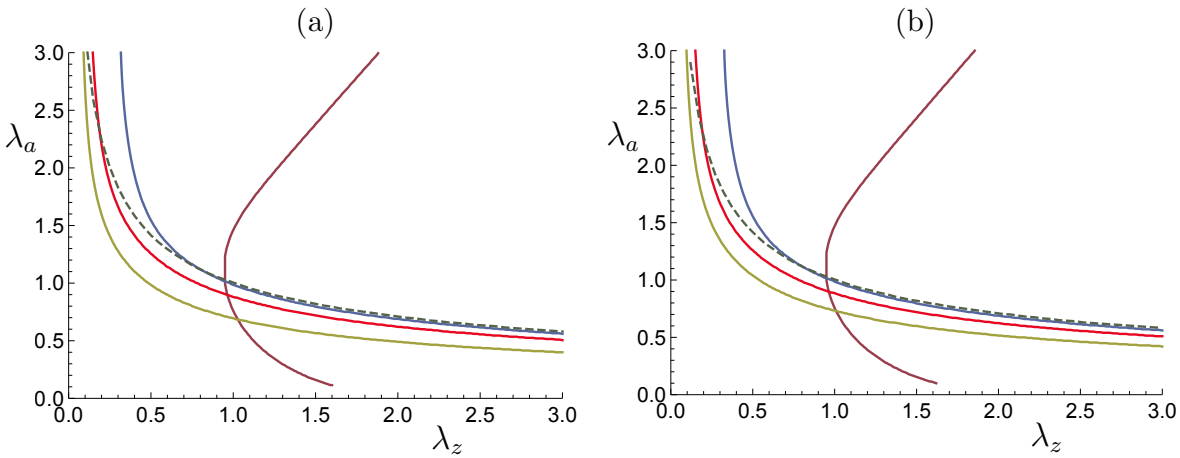

Figure 10: Asymmetric bifurcation curves for $\bar{B} = 1.2$, $\bar{L} = 10$ and $\bar{\kappa} = 0$, with mode numbers $m = 1$ (purple), $m = 2$ (blue), $m = 6$ (red), $m = 10$ (green): (a) $\bar{\nu} = 0$, (b) $\bar{\nu} = 5$. The zero pressure curve is represented by the dashed curve.

Figure 11 provides results for $\bar{B} = 1.2$ with $\bar{\kappa} = 1$ and mode numbers $m = 1, 2, 6, 10$, with $\bar{\nu} = 5$ and $\bar{\nu} = 10$, and corresponding results for $\bar{B} = 1.4$ are shown in Fig. 12. The results for $m = 1$ in Fig. 11 and Fig. 12 for $\bar{\nu} = 5, 10$ are very similar to those for $\bar{\nu} = -5, -10$, which are not shown separately. This is also the case for $m = 2$ and for $m = 6$ when $\bar{B} = 1.2$, while there are some small differences for $m = 6$ when $\bar{B} = 1.4$ and for $m = 10$ with $\bar{B} = 1.2$. Note that in Fig. 11(b) there are additional $m = 6$ and $m = 14$ branches which tend to merge as λ_z increases, and there is also a hint of a lower $m = 1$ branch. Multiple $m = 2, 6, 10$ branches can also be seen in Fig. 12, and different mode priorities emerge under either internal or external pressure depending on the value of λ_z.

For $m = 6$ Fig. 13 illustrates the comparison of plots for $\bar{\nu} = \pm 5$ and $\bar{\nu} = \pm 10$ and Fig. 14 shows the corresponding comparison for $m = 10$. By contrast with the results mentioned above, these figures show that there are some differences between the results for positive and negative $\bar{\nu}$, in particular the appearance of multiple branches for negative $\bar{\nu}$.

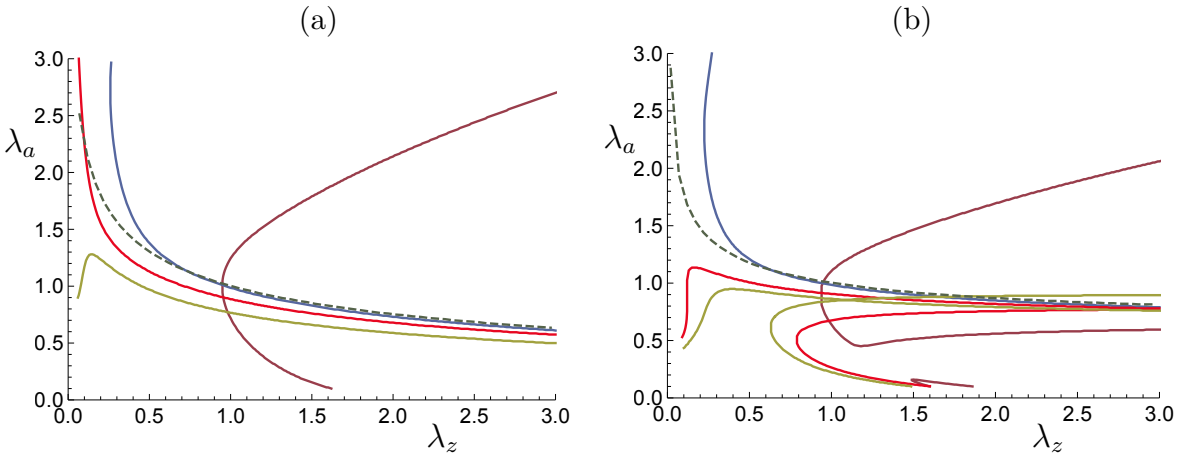

Figure 11: Asymmetric bifurcation curves for $\bar{B} = 1.2$, $\bar{L} = 10$ and $\bar{\kappa} = 1$ with (a) $\bar{\nu} = 5$, (b) $\bar{\nu} = 10$. Mode numbers $m = 1$ (purple), $m = 2$ (blue), $m = 6$ (red), $m = 10$ (green). The zero pressure curve, dependent on $\bar{\nu}$, is represented by the dashed curve.

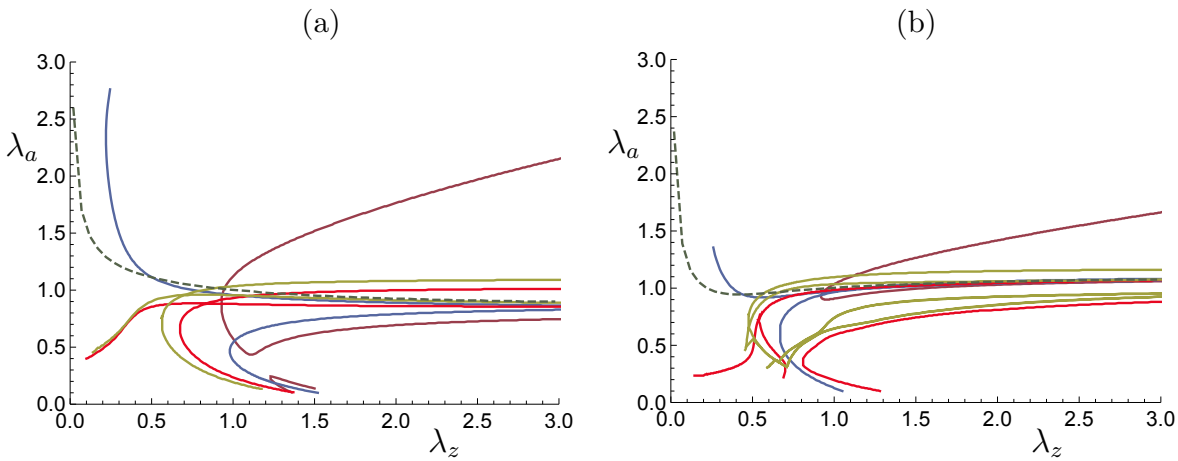

Figure 12: Asymmetric bifurcation curves for $\bar{B} = 1.4$, $\bar{L} = 10$ and $\bar{\kappa} = 1$ with (a) $\bar{\nu} = 5$, (b) $\bar{\nu} = 10$. Mode numbers $m = 1$ (purple), $m = 2$ (blue), $m = 6$ (red), $m = 10$ (green). The zero pressure curve, dependent on $\bar{\nu}$, is represented by the dashed curve.

7 Concluding remarks

The presence of residual stress has a significant influence on the mechanical response and stability of soft solid materials such as biological tissues, including arteries. Inclusion of residual stress in the constitutive description of material response has been established within the framework of the theory of nonlinear elasticity in a number of papers that were referred to in the introductory section. In the present paper we have used this framework and its extension to the theory of incremental elastic deformations superimposed on a finite deformation to study the bifurcation from a circular cylindrical configuration of a deformed residually-stressed tube, under both radial and axial loading. Following the general theory specialized for the considered geometry, the general incremental equations governing bifurcations have been obtained, along with their axisymmetric and prismatic

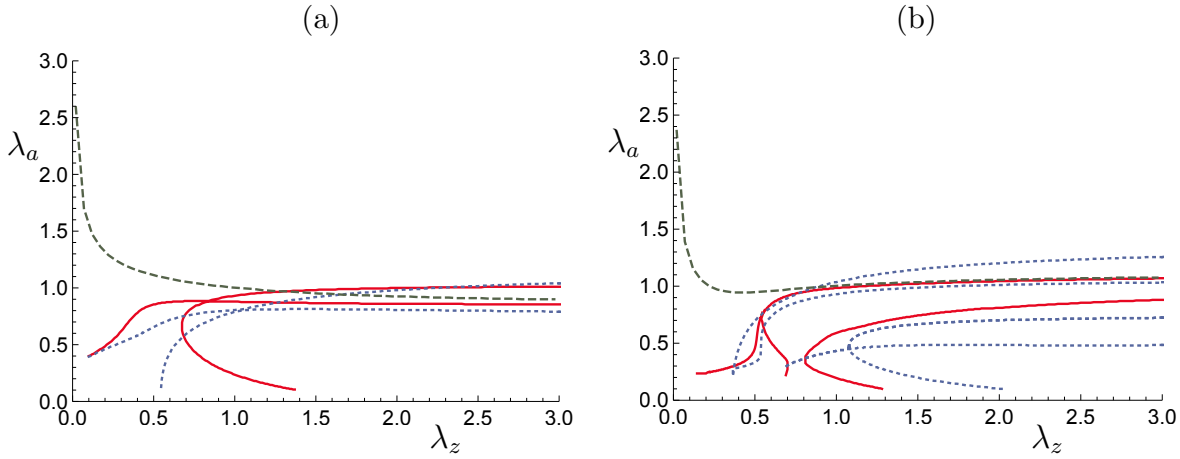

Figure 13: Asymmetric bifurcation curves for $\bar{B} = 1.4$, $\bar{L} = 10$ and $\bar{\kappa} = 1$ with (a) $\bar{\nu} = \pm 5$, (b) $\bar{\nu} = \pm 10$. Mode number $m = 6$. $\bar{\nu} = 5, 10$ (red continuous) and $\bar{\nu} = -5, -10$ (blue dotted). The zero pressure curve, dependent on $\bar{\nu}$, is represented by the dashed curve, but the curves for $\pm\bar{\nu}$ are indistinguishable.

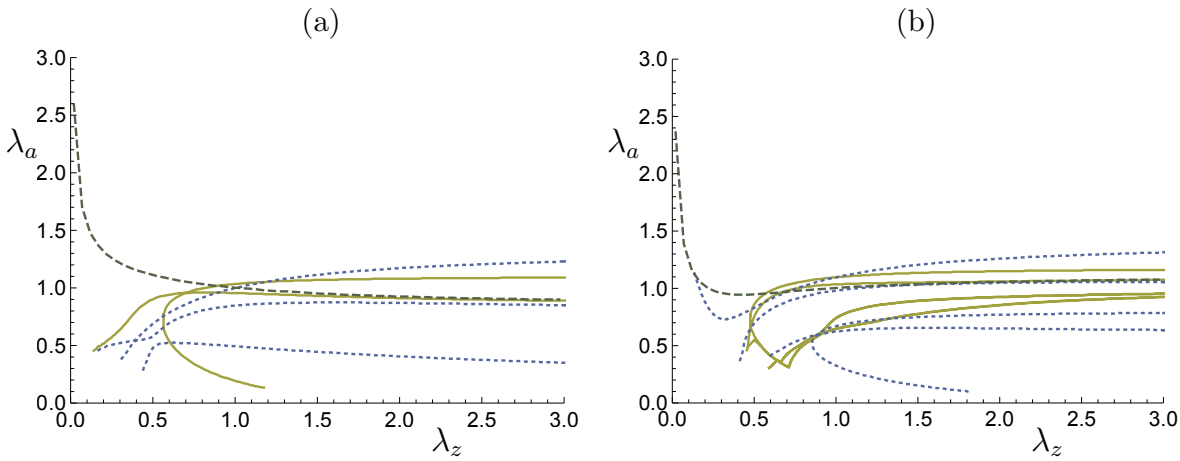

Figure 14: Asymmetric bifurcation curves for $\bar{B} = 1.4$, $\bar{L} = 10$ and $\bar{\kappa} = 1$ with (a) $\bar{\nu} = \pm 5$, (b) $\bar{\nu} = \pm 10$. Mode number $m = 10$. $\bar{\nu} = 5, 10$ (green continuous) and $\bar{\nu} = -5, -10$ (blue dotted). The zero pressure curve, dependent on $\bar{\nu}$, is represented by the dashed curve, but the curves for $\pm\bar{\nu}$ are indistinguishable..

specializations.

The equations have been applied to a prototype constitutive equation that includes a specific form of residual stress that has radial and azimuthal components for purposes of illustrative computations.

Numerical results have been obtained for axisymmetric, prismatic and asymmetric bifurcations and illustrated graphically with an extensive range of examples, including comparison with the case of no residual stress. Depending on the axial stretch and geometrical factors, bifurcation may be triggered by either internal or external pressure, and either axisymmetric, prismatic or asymmetric bifurcations may have priority in either case, depending on the value of λ_z. This can be seen by comparing the axisymmetric,

prismatic and asymmetric results for given parameter values. For example, for $\bar{B} = 1.2$, $\bar{L} = 10$ and $\lambda_z = 1.2$ in Fig. 1 axisymmetric bifurcation (with $m = 0$) can occur under radial expansion ($P > 0$) but not under radial compression ($P < 0$), while with reference to Fig. 6 prismatic bifurcation (independent of $\bar{L}$) does not arise in radial expansion but under radial compression it is possible, first under mode number $m = 2$ close the zero pressure.

Figure 15 exemplifies the dependence of the priorities of the different modes on the deformation. Figure 15(a) shows that the $m = 1$ asymmetric mode only arises for $\lambda_z > 1$, and in the region where $P > 0$ (above the dashed curve) it occurs before the axisymmetric mode (which is independent of m) for the approximate range $(1, 1.12)$ of values of λ_z as P increases from 0. The axisymmetric mode has priority for larger values of λ_z. For $\lambda_z > 1$ the asymmetric mode, but not the axisymmetric mode, is also possible in the region $P < 0$.

For mode number $m = 2$, Fig. 15(b) compares the asymmetric and prismatic bifurcation curves. On the scale shown the $P = 0$ curve (dashed) is virtually indistinguishable from the prismatic bifurcation curve (which is independent of $\bar{L}$). The inset shows the relative disposition of the curves for a selected range of values of λ_z, within which prismatic bifurcation precedes asymmetric bifurcation as P decreases from zero for any fixed value of λ_z shown in the inset. The prismatic bifurcation curve lies entirely below the $P = 0$ curve. However, the asymmetric curve crosses over it as λ_z decreases from 1 and enters the $P > 0$ region. Thus, in axial compression, asymmetric bifurcation can arise under internal pressure. By comparing the blue curves in Figs. 15 (a) and (b) it can be seen that there is a range of values of λ_z where asymmetric bifurcation has priority over axisymmetric bifurcation under inflation, bearing in mind that the axisymmetric curve in Fig. 15(a) is independent of m.

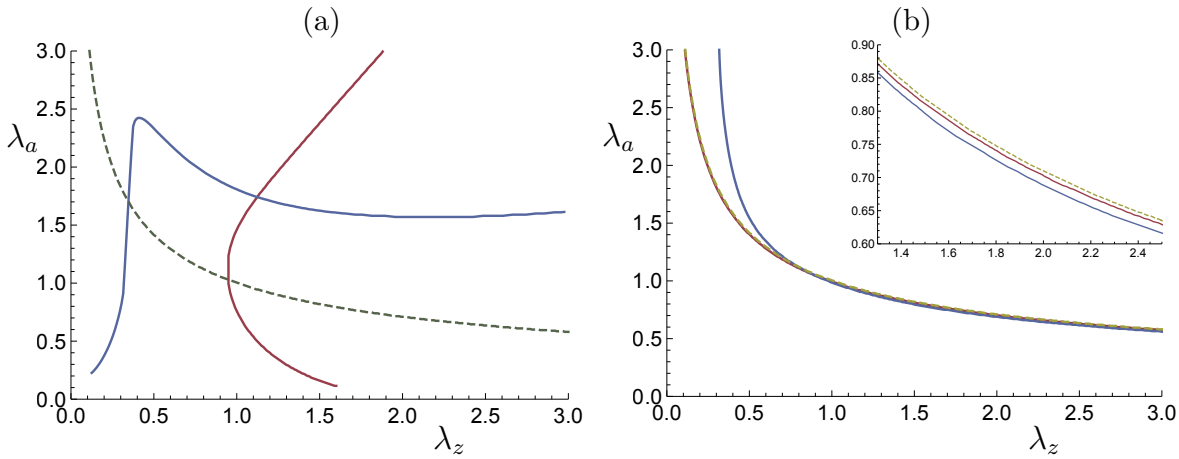

Figure 15: For $\bar{B} = 1.2$, $\bar{\kappa} = 0$, $\bar{\nu} = 0$ and $\bar{L} = 10$: (a) Comparison of the $m = 1$ asymmetric bifurcation curve (purple) and the axisymmetric bifurcation curve (blue) with the zero pressure curve (dashed); (b) for mode number $m = 2$, comparison of the asymmetric (blue) and prismatic (purple) bifurcation curves with the zero pressure curve (dashed). The zoom shows that prismatic bifurcation is possible before asymmetric bifurcation as the pressure decreases from 0 for the considered range of values of λ_z.

The implications of strong ellipticity restrictions for the present geometry have been

examined in Dorfmann and Ogden (2021), in particular the range of values of $\bar{\nu}$, dependent on the geometry and (λ_z, λ_a), for which strong ellipticity holds, regions that have been exemplified in Fig. 5.

In the absence of detailed data quantifying residual stress, in this paper we have restricted attention to a simple, but realistic, form of residual stress and a basic form of constitutive equation. These provide a representative insight into the influence of residual stress on the bifurcation response of a tube and can be refined and generalized when more data become available.

A Appendix: components of $\boldsymbol{\mathcal{A}}_0$

In the general case the components of $\boldsymbol{\mathcal{A}}_0$ are given by

$$
\begin{aligned}
\mathcal{A}_{0piqj} &= 2W_1 B_{pq}\delta_{ij} + 2W_2[I_1 B_{pq}\delta_{ij} - B_{iq}B_{jp} + 2B_{pi}B_{qj} - \delta_{ij}(\mathbf{B}^2)_{pq} - B_{pq}B_{ij}] \\
&+ 2W_5\Sigma_{pq}\delta_{ij} + 2W_6[\Sigma_{pq}B_{ij} + (\boldsymbol{\Sigma}\mathbf{B})_{pq}\delta_{ij} + (\mathbf{B}\boldsymbol{\Sigma})_{pq}\delta_{ij} + \Sigma_{ij}B_{pq} + \Sigma_{pj}B_{iq} + \Sigma_{qi}B_{jp}] \\
&+ 2W_7\Xi_{pq}\delta_{ij} + 2W_8[\Xi_{pq}B_{ij} + (\boldsymbol{\Xi}\mathbf{B})_{pq}\delta_{ij} + (\mathbf{B}\boldsymbol{\Xi})_{pq}\delta_{ij} + \Xi_{ij}B_{pq} + \Xi_{pj}B_{iq} + \Xi_{qi}B_{jp}] \\
&+ 4W_{11}B_{ip}B_{jq} + 4W_{22}B^*_{ip}B^*_{jq} + 4W_{12}[2I_1 B_{ip}B_{jq} - B_{ip}(\mathbf{B}^2)_{jq} - B_{jq}(\mathbf{B}^2)_{ip}] \\
&+ 4W_{15}(B_{ip}\Sigma_{jq} + B_{jq}\Sigma_{ip}) + 4W_{16}[B_{ip}(\boldsymbol{\Sigma}\mathbf{B} + \mathbf{B}\boldsymbol{\Sigma})_{jq} + (\boldsymbol{\Sigma}\mathbf{B} + \mathbf{B}\boldsymbol{\Sigma})_{ip}B_{jq}] \\
&+ 4W_{17}(B_{ip}\Xi_{jq} + B_{jq}\Xi_{ip}) + 4W_{18}[B_{ip}(\boldsymbol{\Xi}\mathbf{B} + \mathbf{B}\boldsymbol{\Xi})_{jq} + (\boldsymbol{\Xi}\mathbf{B} + \mathbf{B}\boldsymbol{\Xi})_{ip}B_{jq}] \\
&+ 4W_{25}(B^*_{ip}\Sigma_{jq} + \Sigma_{ip}B^*_{jq}) + 4W_{26}[B^*_{ip}(\boldsymbol{\Sigma}\mathbf{B} + \mathbf{B}\boldsymbol{\Sigma})_{jq} + (\boldsymbol{\Sigma}\mathbf{B} + \mathbf{B}\boldsymbol{\Sigma})_{ip}B^*_{jq}] \\
&+ 4W_{27}(B^*_{ip}\Xi_{jq} + \Xi_{ip}B^*_{jq}) + 4W_{28}[B^*_{ip}(\boldsymbol{\Xi}\mathbf{B} + \mathbf{B}\boldsymbol{\Xi})_{jq} + (\boldsymbol{\Xi}\mathbf{B} + \mathbf{B}\boldsymbol{\Xi})_{ip}B^*_{jq}] \\
&+ 4W_{55}\Sigma_{ip}\Sigma_{jq} + 4W_{56}[\Sigma_{ip}(\boldsymbol{\Sigma}\mathbf{B} + \mathbf{B}\boldsymbol{\Sigma})_{jq} + (\boldsymbol{\Sigma}\mathbf{B} + \mathbf{B}\boldsymbol{\Sigma})_{ip}\Sigma_{jq}] \\
&+ 4W_{66}(\boldsymbol{\Sigma}\mathbf{B} + \mathbf{B}\boldsymbol{\Sigma})_{ip}(\boldsymbol{\Sigma}\mathbf{B} + \mathbf{B}\boldsymbol{\Sigma})_{jq} \\
&+ 4W_{57}(\Sigma_{ip}\Xi_{jq} + \Xi_{ip}\Sigma_{jq}) + 4W_{67}[(\boldsymbol{\Sigma}\mathbf{B} + \mathbf{B}\boldsymbol{\Sigma})_{ip}\Xi_{jq} + \Xi_{ip}(\boldsymbol{\Sigma}\mathbf{B} + \mathbf{B}\boldsymbol{\Sigma})_{jq}] \\
&+ 4W_{58}[\Sigma_{ip}(\boldsymbol{\Xi}\mathbf{B} + \mathbf{B}\boldsymbol{\Xi})_{jq} + (\boldsymbol{\Xi}\mathbf{B} + \mathbf{B}\boldsymbol{\Xi})_{ip}\Sigma_{jq}] \\
&+ 4W_{68}[(\boldsymbol{\Sigma}\mathbf{B} + \mathbf{B}\boldsymbol{\Sigma})_{ip}(\boldsymbol{\Xi}\mathbf{B} + \mathbf{B}\boldsymbol{\Xi})_{jq} + (\boldsymbol{\Xi}\mathbf{B} + \mathbf{B}\boldsymbol{\Xi})_{ip}(\boldsymbol{\Sigma}\mathbf{B} + \mathbf{B}\boldsymbol{\Sigma})_{jq} \\
&+ 4W_{77}\Xi_{ip}\Xi_{jq} + 4W_{78}[\Xi_{ip}(\boldsymbol{\Xi}\mathbf{B} + \mathbf{B}\boldsymbol{\Xi})_{jq} + (\boldsymbol{\Xi}\mathbf{B} + \mathbf{B}\boldsymbol{\Xi})_{ip}\Xi_{jq}] \\
&+ 4W_{88}(\boldsymbol{\Xi}\mathbf{B} + \mathbf{B}\boldsymbol{\Xi})_{ip}(\boldsymbol{\Xi}\mathbf{B} + \mathbf{B}\boldsymbol{\Xi})_{jq}.
\end{aligned}
$$

The notations

$$\mathbf{B}^* = I_1\mathbf{B} - \mathbf{B}^2, \quad \boldsymbol{\Sigma} = \mathbf{F}\boldsymbol{\tau}\mathbf{F}^{\mathrm{T}}, \quad \boldsymbol{\Xi} = \mathbf{F}\boldsymbol{\tau}^2\mathbf{F}^{\mathrm{T}}$$

are used in the above expressions. In the absence of residual stress only the terms involving $W_1, W_2,\ W_{11}, W_{12}, W_{22}$ are retained, yielding the formula for the components $\mathcal{A}_{0piqj}$ for the standard isotropic specialization.

For the particular model (36) the above components reduce to

$$\mathcal{A}_{0piqj} = \mu B_{pq}\delta_{ij} + \Sigma_{pq}\delta_{ij} + \kappa(I_5 - \operatorname{tr}\boldsymbol{\tau})\Sigma_{pq}\delta_{ij} + 2\kappa\Sigma_{pi}\Sigma_{qj}.$$

B Appendix: components of M

Asymmetric case

$$
\begin{aligned}
\mathsf{M}_{31} &= [r\mathcal{A}'_{03232} - \mathcal{A}_{03232} + m^2\mathcal{A}_{01212} - \alpha^2 r^2(r\mathcal{A}'_{03232} + \mathcal{A}_{03232} \\
&\quad -\mathcal{A}_{01212} - \mathcal{A}_{02222} + \mathcal{A}_{01221} + \mathcal{A}_{01122})]/(r^3\mathcal{A}_{03232}) - mM_{51}/r, \\
\mathsf{M}_{32} &= -[r\mathcal{A}'_{03232} - \mathcal{A}_{03232} - m^2\mathcal{A}_{01212} - \alpha^2 r^2(\mathcal{A}_{02222} - \mathcal{A}_{02233} \\
&\quad -\mathcal{A}_{03223})]/(r^2\mathcal{A}_{03232}) - m\mathsf{M}_{52}/r, \\
\mathsf{M}_{33} &= -(r\mathcal{A}'_{03232} + 2\mathcal{A}_{03232})/(r\mathcal{A}_{03232}), \\
\mathsf{M}_{34} &= [r\mathcal{A}'_{03232} - \mathcal{A}_{03232} + m^2\mathcal{A}_{01212} + \alpha^2 r^2(\mathcal{A}_{02222} - \mathcal{A}_{01221} - \mathcal{A}_{01122})]m/(r^3\mathcal{A}_{03232}) \\
&\quad -m\mathsf{M}_{54}/r \\
\mathsf{M}_{35} &= -(r\mathcal{A}'_{03232} - \mathcal{A}_{03232})m/(r^2\mathcal{A}_{03232}) - m\mathsf{M}_{55}/r, \\
\mathsf{M}_{36} &= \alpha^2/\mathcal{A}_{03232} + m^2/(r^2\mathcal{A}_{03131}).
\end{aligned}
$$

$$
\begin{aligned}
\mathsf{M}_{51} &= (r\mathcal{A}'_{03131} + \mathcal{A}_{03131} + \mathcal{A}_{01111} - \mathcal{A}_{01122} - \mathcal{A}_{02112})m/(r^2\mathcal{A}_{03131}), \\
\mathsf{M}_{52} &= (\mathcal{A}_{01133} - \mathcal{A}_{01122} - \mathcal{A}_{02112} + \mathcal{A}_{03113})m/(r\mathcal{A}_{03131}), \\
\mathsf{M}_{54} &= [r\mathcal{A}'_{03131} + \mathcal{A}_{03131} + m^2(\mathcal{A}_{01111} - \mathcal{A}_{01122} - \mathcal{A}_{02112}) + \alpha^2 r^2\mathcal{A}_{02121}]/(r^2\mathcal{A}_{03131}), \\
\mathsf{M}_{55} &= -(r\mathcal{A}'_{03131} + \mathcal{A}_{03131})/(r\mathcal{A}_{03131}), \\
\mathsf{M}_{56} &= -m/(r\mathcal{A}_{03131}).
\end{aligned}
$$

$$
\begin{aligned}
\mathsf{M}_{61} &= (r\mathcal{A}'_{01133} - r\mathcal{A}'_{02233} - \mathcal{A}_{01111} + \mathcal{A}_{01122} + \mathcal{A}_{03223} - \alpha^2 r^2\mathcal{A}_{02323} - m^2\mathcal{A}_{01313})/r^2, \\
\mathsf{M}_{62} &= (r\mathcal{A}'_{03333} - r\mathcal{A}'_{02233} + r\mathcal{A}'_{03131} - r\mathcal{A}'_{01331} + \mathcal{A}_{03333} - 2\mathcal{A}_{02233} + \mathcal{A}_{01122} \\
&\quad -\mathcal{A}_{03223} - \mathcal{A}_{01313} + \mathcal{A}_{03131})/r, \\
\mathsf{M}_{63} &= \mathcal{A}_{03333} - \mathcal{A}_{02233} - \mathcal{A}_{03223}, \\
\mathsf{M}_{64} &= (r\mathcal{A}'_{01133} - r\mathcal{A}'_{02233} - \mathcal{A}_{01111} + \mathcal{A}_{01122} + \mathcal{A}_{03223} - \mathcal{A}_{01313})m/r^2, \\
\mathsf{M}_{65} &= (\mathcal{A}_{01331} + \mathcal{A}_{01133} - \mathcal{A}_{03223} - \mathcal{A}_{02233})m/r.
\end{aligned}
$$

Axisymmetric case

$$
\begin{aligned}
\mathsf{M}_{41} &= -[-r^2\mathcal{A}''_{03232} + 3r\mathcal{A}'_{03232} - 3\mathcal{A}_{03232} + \alpha^2 r^2(r^2\mathcal{A}''_{03223} + r^2 p'' + r\mathcal{A}'_{03223} + r\mathcal{A}'_{01122} \\
&\quad -r\mathcal{A}'_{01133} - r\mathcal{A}'_{02222} + r\mathcal{A}'_{02233} + \mathcal{A}_{01111} + \mathcal{A}_{02222} - 2\mathcal{A}_{01122} - 2\mathcal{A}_{03223}) \\
&\quad + \alpha^4 r^4\mathcal{A}_{02323}]/(r^4\mathcal{A}_{03232}) \\
\mathsf{M}_{42} &= -[r^2\mathcal{A}''_{03232} - 3r\mathcal{A}'_{03232} + 3\mathcal{A}_{03232} + \alpha^2 r^2(2r\mathcal{A}'_{03223} + 2r\mathcal{A}'_{02233} - r\mathcal{A}'_{02222} \\
&\quad -r\mathcal{A}'_{03333} - \mathcal{A}_{02222} - \mathcal{A}_{03333} + 2\mathcal{A}_{02233} + 2\mathcal{A}_{03223})]/(r^3\mathcal{A}_{03232}) \\
\mathsf{M}_{43} &= -[r^2\mathcal{A}''_{03232} + 3r\mathcal{A}'_{03232} - 3\mathcal{A}_{03232} + \alpha^2 r^2(2\mathcal{A}_{02233} + 2\mathcal{A}_{03223} \\
&\quad -\mathcal{A}_{02222} - \mathcal{A}_{03333})]/(r^2\mathcal{A}_{03232}) \\
\mathsf{M}_{44} &= -2(r\mathcal{A}'_{03232} + \mathcal{A}_{03232})/(r\mathcal{A}_{03232}).
\end{aligned}
$$

Prismatic case

$$
\begin{aligned}
\mathsf{M}_{41} &= -[(m^2-1)(r^2\mathcal{A}''_{03131} + r\mathcal{A}'_{03131} - \mathcal{A}_{03131} + m^2\mathcal{A}_{01313})]/(r^4\mathcal{A}_{03131}) \\
\mathsf{M}_{42} &= -[r^2\mathcal{A}''_{03131} + m^2 r(2\mathcal{A}'_{01133} + 2\mathcal{A}'_{01331} - \mathcal{A}'_{01111} - \mathcal{A}'_{03333}) \\
&\quad + r\mathcal{A}'_{03131} - \mathcal{A}_{03131} + m^2(2\mathcal{A}_{01133} + 2\mathcal{A}_{01331} - \mathcal{A}_{01111} - \mathcal{A}_{03333})]/(r^3\mathcal{A}_{03131}) \\
\mathsf{M}_{43} &= -[r^2\mathcal{A}''_{03131} + 7r\mathcal{A}'_{03131} + 5\mathcal{A}_{03131} \\
&\quad + m^2(2\mathcal{A}_{01133} + 2\mathcal{A}_{01331} - \mathcal{A}_{01111} - \mathcal{A}_{03333})]/(r^2\mathcal{A}_{03131}) \\
\mathsf{M}_{44} &= -2(r\mathcal{A}'_{03131} + 3\mathcal{A}_{03131})/(r\mathcal{A}_{03131}).
\end{aligned} \tag{126}
$$

This research did not receive any specific grant from funding agencies in the public, commercial, or not-for-profit sectors.

References

Ahamed, T., Dorfmann, L., Ogden, R.W., 2016. Modeling of residually stressed material with application to AAA. J. Mech. Behav. Biomed. Mater. 61, 221–234.

Biot, M.A., 1939. Non-linear theory of elasticity and the linearized case for a body under initial stress. Phil. Mag. 27, 468–489.

Biot, M.A., 1940. The influence of initial stress on elastic waves. J. Appl. Phys. 11, 522–530.

Ciarletta, P., Destrade, M., Gower, A.L, Taffetani, M., 2016. Morphology of residually stressed tubular tissues: Beyond the elastic multiplicative decomposition. J. Mech. Phys. Solids 90, 242–253.

Dehghani, H., Desena-Galarza, D., Jha, N.K., Reinoso, J., Merodio, J., 2019. Bifurcation and post-bifurcation of an inflated and extended residually-stressed circular cylindrical tube with application to aneurysms initiation and propagation in arterial wall tissue. Finite Elem. Anal. Des. 161, 51–60.

Dorfmann, L., Ogden, R.W., 2019. Instabilities of soft dielectrics. Phil. Trans. R. Soc. A 377, 20180077.

Dorfmann, L., Ogden, R.W., 2021. The effect of residual stress on the stability of a circular cylindrical tube. J. Eng. Math. 127, 9.

Du, Y., Lu, C., Destrade, M., Chen, W., 2019. Influence of initial residual stress on growth and pattern creation for a layered aorta. Scientific Reports 9, 8232.

Fung, Y.C., 1990. Biomechanics: Motion, Flow, Stress, and Growth, Springer-Verlag, New York.

Haughton, D.M., Ogden, R.W., 1979a. Bifurcation of inflated circular cylinders of elastic material under axial loading—I. Membrane theory for thin-walled tubes. J. Mech. Phys. Solids 27, 179–212.

Haughton, D.M., Ogden, R.W., 1979b. Bifurcation of inflated circular cylinders of elastic material under axial loading—II. Exact theory for thick-walled tubes. J. Mech. Phys. Solids 27, 489–512.

Hoger, A., 1985. On the residual stress possible in an elastic body with material symmetry. Arch. Ration. Mech. Anal. 88, 271–290.

Hoger, A., 1986. On the determination of residual stress in an elastic body. J Elasticity 16, 303–324.

Hoger, A., 1993a. The elasticity tensors of a residually stressed material. J. Elasticity 31, 219–237.

Hoger, A., 1993b. The constitutive equation for finite deformations of a transversely isotropic hyperelastic material with residual stress. J. Elasticity 33, 107–118.

Hoger, A., 1996. The elasticity tensor of a transversely isotropic hyperelastic material with residual stress. J. Elasticity 42, 115–132.

Holzapfel, G.A., Gasser, T.C., Ogden, R.W., 2000. A new constitutive framework for arterial wall mechanics and a comparative study of material models. J. Elasticity 61, 1–48.

Holzapfel, G.A., Ogden, R.W., 2010. Modelling the layer-specific 3D residual stresses in arteries, with an application to the human aorta. J. R. Soc. Interface 7, 787–799.

Johnson, B.E., Hoger, A., 1993. The dependence of the elasticity tensor on residual stress. J. Elasticity 33, 145–165.

Man, C.-S., 1983. Hartig's law and linear elasticity with initial stress. Inv. Prob. 14, 313–319.

Man, C.-S., Lu, W.Y., 1987. Towards an acoustoelastic theory for measurement of residual stress. J. Elasticity 17, 159–182.

Melnikov, A., Ogden, R.W., 2018. Bifurcation of finitely deformed thick-walled electroelastic cylindrical tubes subject to a radial electric field. Zeits. Angew. Math. Phys. 69, 60.

Merodio, J., Haughton, D.M., 2010. Bifurcation of thick-walled cylindrical shells and the mechanical response of arterial tissue affected by Marfan's syndrome. Mech. Res. Comm. 37, 1–6.

Merodio, J., Ogden, R.W., Rodríguez, J., 2013. The influence of residual stress on finite deformation elastic response. Int. J. Non-Lin. Mech. 56, 43–49.

Merodio, J., Ogden, R.W., 2016. Extension, inflation and torsion of a residually-stressed circular cylindrical tube. Cont. Mech. Thermodyn. 28, 157–174.

Ogden, R.W., 1997. Non-linear Elastic Deformations. Dover Publications, New York.

Ogden, R.W., 2003. Nonlinear elasticity, anisotropy, material stability and residual stresses in soft tissue, in: Holzapfel, G.A., Ogden, R.W. (Eds.), Biomechanics of Soft Tissue in Cardiovascular Systems. CISM Courses and Lectures Series 441, pp. 65–108. Springer, Wien.

Ogden, R.W., 2015. Nonlinear elasticity with application to soft fibre-reinforced materials, in: Dorfmann, L., Ogden, R.W. (Eds.), Nonlinear Mechanics of Soft Fibrous Materials. CISM Courses and Lectures Series 559, pp. 1–48. Springer, Wien.

Ogden, R.W., Singh, B., 2011. Propagation of waves in an incompressible transversely isotropic elastic solid with initial stress: Biot revisited. J. Mech. Mater. Struct. 6, 453–477.

Paige, R.E., 2002. FEA in the design process of rubber bushings, in: ABAQUS Users' Conference, pp. 1–15. Simulia, Dassault Systèmes, Providence, RI.

Paige, R.E., Mars, W.V., 2004. Implications of the Mullins effect on the stiffness of a preloaded rubber component, in: ABAQUS Users' Conference, pp. 1–15. Simulia, Dassault Systèmes, Providence, RI.

Rachev, A., 1997. Theoretical study of the effect of stress-dependent remodeling on arterial geometry under hypertensive conditions. J. Biomech. 30, 819–827.

Rachev, A., Hayashi, K., 1999. Theoretical study of the effects of vascular smooth muscle contraction on strain and stress distributions in arteries. Ann. Biomed. Eng. 27, 459–468.

Shams, M., Destrade, M., Ogden, R.W., 2011. Initial stresses in elastic solids: constitutive laws and acoustoelasticity. Wave Motion 48, 552–567.

Shams, M., Ogden, R.W., 2014. On Rayleigh-type surface waves in an initially stressed incompressible elastic solid. IMA J. Appl. Math. 79, 360–376.

Spencer, A.J.M., 1971. Theory of invariants, in: Eringen, A.C. (Ed.), Continuum Physics Vol. 1, pp. 239–353. Academic Press, New York.

Zhu, F., Wu, B., Destrade, M., Chen, W., 2020. Electrostatically tunable axisymmetric vibrations of soft electro-active tubes. J. Sound Vibr. 483, 115467.

Zhu, Y., Luo, X.Y., Ogden, R.W., 2008. Asymmetric bifurcations of thick-walled circular cylindrical elastic tubes under axial loading and external pressure. Int. J. Solids Struct. 45, 3410–3429.

Wolfram Research Inc., 2020. Mathematica 12.1, Champaign, IL.